Soft-Reset Control with Max-of-Quadratics Lyapunov Certificates

R. Bertollo, A.R. Teel, Luca Zaccarian

Soft-Reset Control with Max-of-Quadratics Lyapunov Certificates

R. Bertollo, *Student Member, IEEE*, A.R. Teel, *Fellow, IEEE*, L. Zaccarian, *Fellow, IEEE*

Abstract

We further develop a novel control paradigm encoding the core behavior of a reset control system within a continuous-time feedback, described by a differential inclusion. A tuning knob allows adjusting how close the continuous-time feedback resembles the behavior of the underlying reset controller. The Lyapunov conditions that we derive naturally lead to a sum-of-squares formulation allowing for the design of max-of-quadratics Lyapunov certificates certified by polynomial multipliers. A few application examples confirm the practical effectiveness of the proposed solutions.

Index Terms

Reset control, hybrid systems, stability of hybrid systems, computational methods, computer-aided control design.

I. Introduction

Reset control is a hybrid control strategy that was first introduced by Clegg [1] and later revisited by Horowitz [2] in the context of linear feedback. After a few quiescent decades, the advent of modern representations of hybrid dynamics and hybrid Lyapunov theory generated, in the early 2000, renewed interest in this field (see the surveys in [3], [4]). Among other things, a motivation for reset control is that it has the potential to overcome fundamental limitations of classical feedback laws [5], [6]. Follow-up works essentially branch out in the direction of rigorous Lyapunov-based guarantees for control systems involving reset controllers and continuous-time plants [7]–[9], together with frequency-domain-based studies that are aimed at reducing the gap between theory and control applications [3], [10]. To further motivate and sustain the practical relevance of these techniques, several control applications have been shown to benefit from reset control designs, as testified in [11]–[18], just to cite a few.

A key idea in modern reset control schemes, well described in [7], is to apply an aggressive (possibly exponentially unstable) first-order continuous control action, providing exponentially diverging transients, which is suitably reset to zero in order to obtain hybrid trajectories that exponentially converge to the origin. The stabilizing properties of the controller, known as FORE (first-order reset element), have been thoroughly analyzed in works like [3], [4] and [7].

One of the challenges in tuning these reset controllers is that the resulting trajectories may jump indefinitely, without converging to zero, so some kind of regularization needs to be introduced, as shown in [7], to avoid these nonconverging Zeno phenomena. Moreover, the introduction of the hybrid framework may result in a less intuitive system as compared to classical continuous-time feedback. In the last years, different solutions have been proposed to obtain controllers able to achieve better performance when compared to the well-established linear controllers, while still producing a continuous controller output. In [19], the introduction of a lead-lag pair generates discontinuous state trajectories, but the controller output signals are continuous. In [20], the underlying idea of reset controllers (namely, keeping the sign of the output equal to the sign of the input) is used to propose a new class of controllers known as hybrid integrator-gain systems (HIGS), whose solutions are, by construction, continuous. Lastly, to avoid the need for time regularization, a continuous-time control scheme stemming from a reset control solution, named soft-reset controller, has been proposed in [21] (and further developed in [22]). In [21] it is shown that a weak smooth Lyapunov function, which does not even avoid non-converging Zeno solutions with the reset controller, is already enough to ensure exponential stability of the novel soft-reset scheme.

Following the ideas of [21], in this paper we revisit those results when using nonsmooth functions, which are key for obtaining stability certificates that are not too conservative. In addition, we illustrate here the role of a suitable feedback gain, suggested in [21], that allows modulating the strength of the reset-induced action on the closed-loop system.

Our main results first establish sufficient conditions for global exponential stability of the origin and then show that certain bilinear matrix inequalities (BMI) conditions can be used to provide non-smooth Lyapunov certificates. In particular, we observe that these BMIs are best addressed in association with polynomial multipliers stated as sum of squares (SOS). Indeed, practical experience shows that constant multipliers lead to conditions that are too conservative. This is not surprising, since already in

This work was supported by AFOSR grant FA9550-21-1-0452.

R. Bertollo is with the Department of Industrial Engineering, University of Trento, Trento, Italy (e-mail: riccardo.bertollo@unitn.it).

L. Zaccarian is with LAAS-CNRS, Université de Toulouse, CNRS, Toulouse, France and the Department of Industrial Engineering, University of Trento, Trento, Italy (e-mail: zaccarian@laas.fr).

A.R. Teel is with the Center for Control, Dynamical Systems and Computation. University of California, Santa Barbara, CA 93106, USA (e-mail: teel@ucsb.edu).

[23] it was recognized that stability properties of the homogeneous hybrid dynamics stemming from reset control mechanisms are best addressed with the use of nonquadratic certificates (such as homogeneous higher order polynomials as in [23]). Similar observations can also be found in [24].

To solve our BMI-max-of-quadratics formulations we propose an iterative sum-of-squares algorithm that constructs such nonsmooth Lyapunov functions. The iterative part of the algorithm is inspired by the path-following technique proposed in [25]. The SOS certificates allow using polynomial multipliers in our BMI conditions, resulting in a less conservative equivalent formulation.

The paper is organized as follows: in Section II we introduce some preliminary results on non-smooth strongly convex functions. In Section III we present the soft-reset closed loop, and we state and prove asymptotic stability of the continuous-time dynamics with nonsmooth Lyapunov certificates. In Section IV we identify BMI conditions with polynomial multipliers, which ensure the main stability result using a max-of-quadratics Lyapunov function and SOS constraints. In Section V we present an iterative algorithm to construct these max-of quadratics Lyapunov certificates. Lastly, in Section VI we present an application of our work to a second-order system, resembling the dynamics of a class of mechatronic systems.

Notation: $|x| := \sqrt{x^\top x}$ denotes the Euclidean norm; $\mathcal{B}_r(x) \subset \mathbb{R}^n$ denotes a ball of radius $r > 0$ centered at $x \in \mathbb{R}^n$; $\mathbb{S}^{n-1} \subset \mathbb{R}^n$ denotes the unit sphere in $\mathbb{R}^n$; $\lambda_{\mathrm{m}}(P)$ denotes the minimum eigenvalue of a symmetric matrix P, while $\lambda_{\mathrm{M}}(P)$ denotes its maximum eigenvalue.

II. Preliminaries on non-smooth strongly convex functions

As a preliminary mathematical background, we recall here some properties of non-smooth strongly convex functions, which are well known in the smooth case [26]. Due to [26, Lemma 3.1.2] and [27, Prop. 2.2.6], nonsmooth convex functions are Lipschitz in the interior of their domain. To rule out the defective cases of [26, Ex. 3.1.1(6) and 3.1.2(4)] we consider functions $W : \mathbb{R}^n \to \mathbb{R}$ with $\mathrm{dom} W = \mathbb{R}^n$, so that convexity implies Lipschitz continuity.

We recall that a function $W : \mathbb{R}^n \to \mathbb{R}$ is *convex* (and Lipschitz) if, for each x_1 and x_2 in $\mathbb{R}^n$, we have

$$W\left(tx_1 + (1-t)x_2\right) \leq tW\left(x_1\right) + (1-t)\,W\left(x_2\right),\ \forall t \in [0,1]\,,$$

and that a function V is *strongly convex with parameter* $\eta > 0$ when $x \mapsto W(x) := V(x) - \frac{\eta}{2} x^\top x$ is convex.

For a convex function $V : \mathbb{R}^n \to \mathbb{R}$, which is not necessarily differentiable, instead of the gradient, we use the *subdifferential* ∂V of V: a set-valued map defined as follows

$$\partial V(x) := \{\zeta_v \in \mathbb{R}^n : V(y) - V(x) \geq \langle \zeta_v, y - x\rangle, \forall y \in \mathbb{R}^n\}.$$

While the above is the standard definition of subdifferential, in this paper we use the following equivalent definition stemming from the *Clarke generalized gradient* [27], which is also defined for nonconvex Lipschitz functions[1]:

$$\partial V(x) := \mathrm{co}\{\lim_{i\to\infty} \nabla V(x_i) :\ x_i \to x, x_i \notin \mathcal{S}\}, \tag{1}$$

where $\mathrm{co}(\cdot)$ denotes the convex hull and $\mathcal{S} \subset \mathbb{R}^n$ is any set of measure zero including the points where V is not differentiable (due to Rademacher's theorem, V is differentiable everywhere except possibly on a set of measure zero). We use here formalism (1), because it allows stating Lemma 2 and Lemma 3 in a more general way, so that the results may be extended to nonconvex functions in the future (see Remark 3 at the end of Section III).

The following lemma is an extension of [26, Definition 2.1.2] to the Lipschitz case. The same result is also presented in [28, Lemma 2]. A proof is reported here for completeness.

Lemma 1: A Lipschitz function $V : \mathbb{R}^n \to \mathbb{R}$ is strongly convex with parameter $\eta > 0$ if and only if

$$V(y) \geq V(x) + \langle \zeta_v, y - x\rangle + \frac{\eta}{2}|y-x|^2,\ \forall \zeta_v \in \partial V(x), \tag{2}$$

for all $(x, y) \in \mathbb{R}^n \times \mathbb{R}^n$.

Proof: From [29, Cor. 2.6(c)], strong convexity of V implies that, for all $x, y \in \mathbb{R}^n$,

$$W(y) \geq W(x) + \langle \zeta_W, y - x\rangle, \forall \zeta_W \in \partial W(x). \tag{3}$$

The converse is also true. Indeed, pick any $y_1, y_2 \in \mathbb{R}^n$ and for any $\lambda \in [0, 1]$ we may select $x = \lambda y_1 + (1-\lambda)y_2$ and evaluate (3) for $y = y_1$ and $y = y_2$ to get, for all $\zeta_W \in \partial W(x)$,

$$\begin{aligned} W(y_1) &\geq W(x) + \langle \zeta_W, y_1 - x\rangle, \\ W(y_2) &\geq W(x) + \langle \zeta_W, y_2 - x\rangle. \end{aligned}$$

[1]The equivalence between (1) and the subdifferential, for convex Lipschitz functions, is established in [27, Prop 2.2.7 and Thm 2.5.1].

Multiplying the first inequality by λ and the second one by $(1-\lambda)$ and summing up, we get

$$\begin{aligned}\lambda W(y_1) + (1-\lambda)W(y_2) &\\ &\geq W(x) + \langle \zeta_w, \lambda y_1 + (1-\lambda)y_2 - x\rangle \\ &\geq W(x) + \langle \zeta_w, 0\rangle = W(\lambda y_1 + (1-\lambda)y_2),\end{aligned}$$

which is the definition of convexity.

Summarizing, we have proven that V is strongly convex if and only if (3) holds for all $x, y \in \mathbb{R}^n$.

Continuing, apply [27, Prop. 2.3.3, p. 38] and [27, Cor. 1, p. 39], to get that $\partial W(x) = \partial V(x) - \eta x$. Therefore (3) is equivalent to $V(y) - \frac{\eta}{2} y^\top y \geq V(x) - \frac{\eta}{2} x^\top x + \langle \zeta_V - \eta y, y - x\rangle$, for all $\zeta_V \in \partial V(x)$. Rearranging terms, this corresponds to (2). ■

Remark 1: We emphasize that condition (3) can be equivalently written as

$$V(y) \geq V(x) + \langle \nabla V(x), y - x\rangle + \frac{\eta}{2}|y-x|^2. \tag{4}$$

for almost all $(x, y) \in \mathbb{R}^n \times \mathbb{R}^n$. The fact that (2) implies (4) is trivial. The opposite implication holds because of the definition in (1). In particular, assume that (4) holds almost everywhere. Then for each $x, y \in \mathbb{R}^n$, consider any sequence of points where x_i where V is differentiable, such that $x_i \to x$ and $\zeta_i = \nabla V(x_i) \to \zeta^\star \in \partial V(x)$. From the continuity of V, (2) holds with $\zeta_v = \zeta^\star$. Moreover, (2) also holds for any ζ_v in the convex hull of any such limiting value $\zeta^\star$, due to linearity of (2) with respect to ζ_v. •

III. Continuous-time implementation of reset control

A. Dynamics and main stability result

Consider the following homogeneous hybrid dynamical system with state $x \in \mathbb{R}^n$:

$$\mathcal{H} \quad \begin{cases} \dot{x} &= Ax, \qquad x \in \mathcal{C}, \\ x^+ &= Rx, \qquad x \in \mathcal{D}, \end{cases} \tag{5}$$

where the flow and jump sets are defined as

$$\begin{aligned}\mathcal{C} &:= \{x \in \mathbb{R}^n : x^\top M x \leq 0\} \\ \mathcal{D} &:= \{x \in \mathbb{R}^n : x^\top M x \geq 0\},\end{aligned} \tag{6}$$

with $A, R, M \in \mathbb{R}^{n\times n}$, and $M = M^\top$.

Based on the preliminary results of [21], the purpose of this work is to certify, using non-smooth Lyapunov functions, exponential stability for a continuous-time implementation of the hybrid reset control system (5)-(6), known as soft-reset system. To this end, we assume that the hybrid data of the original system satisfy the following assumption.

Assumption 1: For system (5)-(6), there exists a Lipschitz, homogeneous of degree two, positive definite function $V : \mathbb{R}^n \to \mathbb{R}$ such that

(i) V is strongly convex

(ii) there exist $\varepsilon > 0$ such that, defining $\mathcal{C}_\varepsilon := \{x \in \mathbb{R}^n : x^\top M x \leq \varepsilon x^\top x\}$, the following holds:

$$\langle \nabla V(x), Ax\rangle \leq 0, \quad \text{for almost all } x \in \mathcal{C}_\varepsilon, \tag{7}$$

$$V(Rx) - V(x) \leq 0, \quad \text{for all } x \in \mathcal{D}; \tag{8}$$

(iii) $x \in \mathcal{D}$ implies $Rx \in \mathcal{C}$;

(iv) no continuous solution to (5)-(6) exists that keeps V constant and nonzero.

■

Item (ii) of Assumption 1 ensures only stability of the origin for (5)-(6); items (iii) and (iv) do not give any guarantee of the origin's attractivity. Attractivity fails when a system allows for discrete nonzero solutions that keep V (defined in Assumption 1) constant and nonzero. This happens in many reset control systems, and the issue is typically resolved by the introduction of some kind of time or space regularization,see, e.g., the discussion in [7, Section I] and references therein. Simplifying the implementation is one of the motivations for introducing, in [21], the following continuous-time system, inspired by the essential nature of the solutions of (5)-(6):

$$\dot{x} \in F(x) := Ax + \gamma \Big(\mathrm{SGN}\left(x^\top M x\right) + 1 \Big)\left(Rx - x\right), \tag{9}$$

with $\gamma > 0$ sufficiently large. The continuous-time dynamics (9) is a differential inclusion because of the set-valued mapping $\mathrm{SGN} : \mathbb{R} \rightrightarrows \mathbb{R}$, defined as

$$\mathrm{SGN}(x) := \begin{cases} x/|x|, & \text{if } x \neq 0, \\ [-1, 1], & \text{if } x = 0. \end{cases} \tag{10}$$

Consequently, the set-valued mapping F in (9) is outer semicontinuous and locally bounded with convex values.

Remark 2: As noted in [21], (9) is equivalent to (5) when x belongs to the interior of $\mathcal{C}$ in (6). Indeed, when $x^\top Mx < 0$, $F(x) = Ax$. On the other hand, when x belongs to the interior of $\mathcal{D}$ and $\gamma \to \infty$, we have $F(x) \approx 2\gamma(Rx - x)$, which corresponds to a continuous-time approximation of the jump map in (5). Summarizing, the selection of γ allows tuning how accurately the solutions of (9) approximate the projection on the continuous-time axis of the hybrid solutions of (5)-(6). • Following the proof technique of [21], suitably generalized to the Lipschitz case, we can show here that this soft-reset dynamics ensures global exponential stability of the origin even when the original hybrid system does not have an attractive origin. In particular, the following holds.

Theorem 1: Under Assumption 1, the origin of (9) is globally exponentially stable for $\gamma > 0$ sufficiently large. Moreover, if (7) holds for almost all $x \in \mathbb{R}^n$, then the origin of (9) is globally exponentially stable for any $\gamma > 0$.

Note that item (iii) of Assumption 1 is reasonable when transitioning to a continuous-time implementation as in (9), since it would not make sense to do so starting from a purely discrete system. Additionally, (7) together with item (iv) are typical convergence guarantees for the continuous-time part of the hybrid system (5), although we emphasize once again that Assumption 1 does not guarantee asymptotic stability of the origin for the hybrid system (5)-(6).

Some conditions that might appear strict are requiring that (7) holds on $\mathcal{C}_\varepsilon$ and the strong convexity assumption on V in item (i) of Assumption 1. Asking that (7) holds on a slightly inflated version of $\mathcal{C}$ is a means of guaranteeing some robustness that is needed to pass from the hybrid implementation to the continuous-time implementation, as it will be clear in the proof of Theorem 1. Lastly, the strong convexity assumption in item (i) can be removed by working with a direct Lyapunov construction for the soft-reset dynamics. This last aspect is discussed in Remark 3.

B. Proof of Theorem 1

For the proof of Theorem 1, we rely on the following lemmas providing two useful estimates of the generalized directional derivative of V in the direction Ax.

Lemma 2: Under item (ii) of Assumption 1, the following holds

$$\langle v, Ax \rangle \leq 0, \quad \forall x \in \mathcal{C}_{\frac{\varepsilon}{2}}, \ \forall v \in \partial V(x). \tag{11}$$

Proof: For $x = 0$, inequality (11) holds trivially. Moreover, for each $x \in \mathbb{R}^n \setminus \{0\}$ satisfying $x^\top Mx \geq \frac{\varepsilon}{2}|x|^2$, it is immediate to verify that any x_i in the ball $\mathcal{B}_{\delta(x)}(x)$ having radius $\delta(x) := \frac{\varepsilon}{3(\varepsilon+2|M|)}|x|$, satisfies $x_i^\top Mx_i \leq \varepsilon|x_i|^2$. This implies, from (7) in Assumption 1,

$$\langle \nabla V(x_i), Ax_i \rangle \leq 0, \ \text{for almost all } x_i \in \mathcal{B}_{\delta(x)}(x). \tag{12}$$

Based on the definition in (1), consider any sequence $x_i \to x$ contained in $\mathcal{B}_{\delta(x)}(x)$ and satisfying $\nabla V(x_i) \to v^\star$ in addition to the left bound in (12). Due to the Lipschitz properties of V, for each x there exists L such that $|\nabla V(z)| \leq L$ for almost all $z \in \mathcal{B}_{\delta(x)}(x)$. This implies $|\lim_{i\to\infty} \langle \nabla V(x_i), A(x_i - x) \rangle| \leq \lim_{i\to\infty} L|A||x_i - x| = 0$. Using this last inequality and (12), we get

$$\begin{aligned} \langle v^\star, Ax \rangle &= \lim_{i\to\infty} \langle \nabla V(x_i), Ax \rangle + \langle \nabla V(x_i), A(x_i - x) \rangle \\ &= \lim_{i\to\infty} \langle \nabla V(x_i), Ax_i \rangle \leq 0. \end{aligned}$$

Finally, note that linearity of the scalar product $\langle v^\star, Ax \rangle$ allows extending the bound above to any convex combination of such limit vectors $v^\star$, namely to any vector $v \in \partial V(x)$, as to be proven. ■

Lemma 3: Under item (ii) of Assumption 1, the constant $\kappa := \sup_{|\bar{x}|=1, \ v\in\partial V(\bar{x})} \langle v, A\bar{x} \rangle$ is finite and satisfies

$$\langle v, Ax \rangle \leq \kappa |x|^2, \quad \forall x \in \mathbb{R}^n, \forall v \in \partial V(x). \tag{13}$$

Proof: The constant κ is finite since ∂V is locally bounded, due to (1) and the fact that ∇V is locally bounded since V is locally Lipschitz.

To the end of proving (13) for $x \neq 0$ (for $x = 0$ it holds by inspection), consider the expression of the generalized directional derivative $V^\circ(x; Ax)$ given in [27, p. 10, eqs (1), (3)] and note that for each $x \neq 0$, defining $\bar{x} := \frac{x}{|x|}$, using the homogeneity

(of degree two) of V, we have

$$\begin{aligned}\max_{v\in\partial V(x)}\langle v, Ax\rangle &= V^\circ(x;Ax)\\ &= \limsup_{y\to x, h\searrow 0}\frac{V(y+hAx)-V(y)}{h}\\ &= \limsup_{\bar y\to \bar x, h\searrow 0}\frac{V(|x|\bar y+hA|x|\bar x)-V(|x|\bar y)}{h}\\ &= |x|^2\limsup_{\bar y\to \bar x, h\searrow 0}\frac{V(\bar y+hA\bar x)-V(\bar y)}{h}\\ &= |x|^2\max_{v\in\partial V(\bar x)}\langle v, A\bar x\rangle \le \kappa|x|^2,\end{aligned}$$

as to be proven. ■

By also using the results in Section II, we are now ready to prove Theorem 1; our proof generalizes the main result in [21] to the case where the Lyapunov function is non-smooth.

Proof of Theorem 1. It is straightforward to see that $F(\lambda x)=\lambda F(x)$ for all $\lambda>0$ and $x\in\mathbb{R}^n$. Hence global exponential stability of the origin is equivalent to asymptotic stability of the origin; see [30, Theorem 11], for example. It remains to prove asymptotic stability of the origin, namely Lyapunov stability + global attractivity, which are proven below.

A. Lyapunov Stability. Let us first focus on proving Lyapunov stability. From Lemma 1, the strong convexity assumed initem (i) of Assumption 1 implies that there exists $\eta>0$ satisfying (2). Take $x=0$ in (2) and note that $V(y)$ is lower bounded by a quadratic form in y where the quadratic term is $\frac{\eta}{2}|y|^2$. This implies radial unboundedness, which implies that V has compact sublevel sets. Using the results in [29, §4.5] it is straightforward to check that Lyapunov stability of the origin for $\dot x\in F(x)$ is guaranteed if there exists a locally Lipschitz function V positive definite and having compact sublevel sets, such that

$$|x|\neq 0 \;\Rightarrow\; \langle v, f\rangle\le 0,\quad \forall f\in F(x), \forall v\in\partial V(x). \tag{14}$$

To the end of proving (14), let us break the analysis into three main steps.

Step A.1: Bounding $\langle \partial V(x), \big(\text{SGN}(x^\top Mx)+1\big)(Rx-x)\rangle$.

Select $y=Rx$ in (2) (which holds due to the strong convexity assumption) and using (8) and the definition of D in (6), we have for all $x\neq 0$ and for all $v\in\partial V(x)$,

$$x^\top Mx\ge 0 \quad\Longrightarrow\quad \langle v, Rx-x\rangle\le -\frac{\eta}{2}|Rx-x|^2. \tag{15}$$

Exploiting linearity of the scalar product, and from the definition of SGN in (10), the previous inequality implies that for all $x\neq 0$, for all $v\in\partial V(x)$ and for all $s\in\text{SGN}(x^\top Mx)$,

$$\langle v, (s+1)(Rx-x)\rangle\le -(s+1)\frac{\eta}{2}|Rx-x|^2. \tag{16}$$

Letting $\sigma>0$ satisfy $|M(Rx+x)|\le\sigma|x|$ for all $x\in\mathbb{S}^{n-1}$, and then using the Cauchy-Schwarz inequality, item (iii) in Assumption 1, and $M=M^\top$, it follows that for all $x\neq 0$

$$\begin{aligned}x^\top Mx\ge 0 \quad\Rightarrow\quad |Rx-x| &\ge \frac{-(Rx-x)^\top M(Rx+x)}{\sigma|x|}\\ &= \frac{x^\top Mx - x^\top R^\top MRx}{\sigma|x|}\\ &\ge \frac{x^\top Mx}{\sigma|x|}\ .\end{aligned} \tag{17}$$

Combining (16) and (17) results in

$$\langle v, (s+1)(Rx-x)\rangle\le -\eta\max\big\{0, x^\top Mx\big\}\,\frac{x^\top Mx}{\sigma^2|x|^2}, \tag{18}$$

for all $x\neq 0$, all $v\in\partial V(x)$ and all $s\in\text{SGN}(x^\top Mx)$.

Step A.2: Bounding $\langle\partial V(x), Ax\rangle$.

For each $x\in\mathbb{R}^n\setminus\{0\}$ satisfying $x^\top Mx\le\frac{\varepsilon}{2}|x|^2$, Lemma 2 establishes the bound

$$x^\top Mx\le\frac{\varepsilon}{2}|x|^2 \;\Rightarrow\; \langle v, Ax\rangle\le 0,\quad\forall v\in\partial V(x). \tag{19}$$

For the remaining points, which satisfy $x^\top Mx \geq \frac{\varepsilon}{2}|x|^2$, we use (13) of Lemma 3 to obtain, for all $v \in \partial V(x)$,

$$x^\top Mx \geq \frac{\varepsilon}{2}|x|^2 \;\Rightarrow\; \langle v, Ax\rangle \leq \kappa|x|^2 \leq \frac{2\kappa}{\varepsilon}x^\top Mx \leq \max\left\{0, x^\top Mx\right\}\frac{4\kappa\sigma^2}{\varepsilon^2}\frac{x^\top Mx}{\sigma^2|x|^2}. \tag{20}$$

Step A.3: Wrapping up.

It follows from (19) and (20) together with (18) that, for each $\nu > 0$ there exists $\gamma > 0$ sufficiently large, such that for all $x \neq 0$,

$$\langle v, Ax + \gamma \cdot (s+1)(Rx - x)\rangle \leq -\nu \max\left\{0, x^\top Mx\right\}\frac{x^\top Mx}{|x|^2} \leq 0, \tag{21}$$

for all $v \in \partial V(x)$ and all $s \in \text{SGN}(x^\top Mx)$. This clearly implies (14) and shows Lyapunov stability of the origin for (9). Consider now the case where (7) holds for almost all $x \in \mathbb{R}^n$. Then bound (19) holds everywhere and there is no need to use bound (20). As a consequence, combining (18) and (19), we obtain (21) with $\nu = \frac{\eta}{\sigma^2}$ for any value of $\gamma > 0$. This implies, once again, (14) and therefore Lyapunov stability.

Global Convergence. To prove convergence, we apply the invariance principle for differential inclusions in [31, Thm 2.11], which applies due to the properties of F listed below (10). In particular, the origin is globally attractive if and only if there is no solution $x : \mathbb{R}_{\geq 0} \to \mathbb{R}^n$ and $c > 0$ such that $V(x(t)) = c$ for all $t \geq 0$. Being a solution of (9), $x(\cdot)$ satisfies, for almost all t,

$$\dot{x}(t) = Ax(t) + \gamma \cdot (s(t)+1)(Rx(t) - x(t)), \tag{22a}$$

$$s(t) \in \text{SGN}\left(x^\top(t)Mx(t)\right). \tag{22b}$$

Assuming that $t \mapsto V(x(t))$ is a non-zero constant, by the generalized chain rule presented in [32] (see also [33, Prop. 4]), for almost all t,

$$0 = \langle v(t), Ax(t) + \gamma \cdot (s(t)+1)(Rx(t) - x(t))\rangle, \tag{23}$$

for some $v(t) \in \partial V(x(t))$. According to (21), such a solution requires $x^\top(t)Mx(t) \leq 0$ for all $t \geq 0$. In turn, it follows from (20) and (16) and the positivity of γ that, for almost all t,

$$0 = \langle v(t), Ax(t)\rangle \tag{24a}$$

$$0 = \langle v(t), \gamma \cdot (s(t)+1)(Rx(t) - x(t))\rangle. \tag{24b}$$

Again with (16) and the positivity of γ and η, it follows that, for almost all t,

$$(s(t)+1)|Rx(t) - x(t)|^2 = 0. \tag{25}$$

It then follows from (22a) that $\dot{x}(t) = Ax(t)$ for almost all t, namely $x(\cdot)$ is also a solution of (5)-(6). In turn, it follows from item (iv) of Assumption 1 that $x(\cdot)$ does not keep V equal to a nonzero constant. That is, $V(x(t)) = c > 0$ for all $t \in \mathbb{R}_{\geq 0}$ is impossible. □

Remark 3: The strong convexity hypothesis in item (i) and equation (8) in item (ii) of Assumption 1 are used only once in the proof of Theorem 1. In particular, these two conditions combined are used to prove inequality (15). For this reason, a relaxed version of Assumption 1, not requiring strong convexity of the Lyapunov function, could be obtained by directly assuming (15). Starting from this relaxed assumption, one could proceed as in the next sections and generate an alternative (iterative) algorithm, imposing a numerically tractable sufficient condition for (15) for the synthesis of a nonconvex max of quadratics Lyapunov function. However, preliminary attempts to do so led to sufficient conditions that are too conservative and therefore ineffective. Thus, we regard these challenging directions as future work. •

IV. Max of quadratics Lyapunov functions with SOS multipliers

With quadratic Lyapunov functions, the conditions in item (ii) of Assumption 1 are either trivially satisfied or they can be verified through linear algebra. However, they often lead to conservative results, see [34, Example 1]. Moreover, for certain reset control feedbacks it is known that no quadratic Lyapunov function exists certifying internal stability (see, for example, the discussion in [8, page 1142]).

To address this issue, we propose here an approach for checking Assumption 1 with max of quadratics Lyapunov functions. Given q matrices $P_i = P_i^\top, i \in \mathcal{Q} := \{1, \ldots, q\}$, a max of quadratics function is defined as

$$V(x) := \max_{i \in \mathcal{Q}} x^\top P_i x. \tag{26}$$

We show below that, for ensuring selected properties in Assumption 1, it is enough to search for constants $\alpha \geq 0$, $\beta \geq 0$, $\varepsilon > 0$, $\bar{\varepsilon} > 0$, polynomial functions $r_{i\Lambda}$, r_{iS}, r_{iF}, r_{iJ}, and SOS polynomials τ_{ij}, μ_{i0}, μ_{ij}, λ_{i0}, λ_{ij} such that, for all $i \in \mathcal{Q}$, the polynomials

$$\begin{aligned} S_i(x) &:= x^\top P_i x - \sum_{j=1}^{q} \tau_{ij}(x) x^\top (P_i - P_j) x \\ &\quad + r_{iS}(x)(1 - x^\top x) - \bar{\varepsilon} x^\top x, \end{aligned} \tag{27a}$$

$$\begin{aligned} F_i(x) &:= -x^\top (P_i A + A^\top P_i) x - \sum_{j=1}^{q} \mu_{ij}(x) x^\top (P_i - P_j) x \\ &\quad + \mu_{i0}(x) x^\top (M - \varepsilon I) x + r_{iF}(x)(1 - x^\top x) - 2\alpha x^\top P_i x, \end{aligned} \tag{27b}$$

$$\begin{aligned} J_i(x) &:= -x^\top R^\top P_i R x + \mathrm{e}^{-2\beta} \sum_{j=1}^{q} \lambda_{ij}(x) x^\top P_j x \\ &\quad - \lambda_{i0}(x) x^\top M x + r_{iJ}(x)(1 - x^\top x), \end{aligned} \tag{27c}$$

$$\Lambda_i(x) := 1 - \sum_{j=1}^{q} \lambda_{ij}(x) + r_{i\Lambda}(x)(1 - x^\top x), \tag{27d}$$

are all SOS.

Proposition 1: Assume that there exist q symmetric matrices P_i, constants $\alpha \geq 0$, $\beta \geq 0$, $\varepsilon > 0$, polynomials $r_{i\Lambda}$, r_{iS}, r_{iF}, r_{iJ}, and SOS polynomials τ_{ij}, μ_{i0}, μ_{ij}, λ_{i0}, λ_{ij} such that, for all $i \in \mathcal{Q}$, all of the polynomials in (27) are SOS. Then function V in (26) satisfies (7), (8), and, if $\alpha > 0$, item (iv) of Assumption 1 holds too. Finally, if $P_i > 0$ for all $i \in \mathcal{Q}$, then V is strongly convex and satisfies item (ii) of Assumption 1.

Remark 4: The SOS certificates obtained with polynomial multipliers are a generalization of the BMI conditions that one could obtain using the S-procedure and constant multipliers. Moreover, if matrices P_i are fixed, the conditions become LMIs arising from SOS representations of the polynomial multipliers. This fact may be exploited when wanting to verify selected properties of Assumption 1 for a given Lyapunov function V. Constant multipliers are more intuitive and widely used in the literature, but we discuss in Remark 5 that in many cases they prove to be too conservative in this formulation, probably because of the repeated use of the lossy S-procedure. •

To prove Proposition 1, we first establish a few convenient properties for the function V.

Lemma 4: Under the hypotheses of Proposition 1, there exist positive scalars c_1, c_2 such that function V in (26) satisfies

$$c_1 |x|^2 \leq V(x) \leq c_2 |x|^2, \qquad \text{for all } x \in \mathbb{R}^n, \tag{28a}$$

$$\langle \nabla V(x), Ax \rangle \leq -2\alpha V(x), \qquad \text{for almost all } x \in \mathcal{C}_\varepsilon, \tag{28b}$$

$$V(Rx) \leq \mathrm{e}^{-2\beta} V(x), \qquad \text{for all } x \in \mathcal{D}. \tag{28c}$$

Proof: We prove the three inequalities in (28) one by one.

Proof of SOS of (27a) $\implies$ (28a). Let us first consider any $x \in \mathbb{R}^n$ with $|x| = 1$. Then, the term $(1 - x^\top x)$ in (27a) becomes zero, and since the polynomial is SOS, we have

$$x^\top P_i x - \sum_{j=1}^{q} \tau_{ij}(x) x^\top (P_i - P_j) x - \bar{\varepsilon} x^\top x \geq 0.$$

Consider now any $i \in \mathcal{Q}$ such that $V(x) = x^\top P_i x \geq x^\top P_j x, \forall j \in \mathcal{Q}$. Then the previous inequality, together with $\tau_{ij} \geq 0$ and $\bar{\varepsilon} > 0$, yields $V(x) = x^\top P_i x > \sum_{j=1}^{q} \tau_{ij}(x) x^\top (P_i - P_j) x \geq 0$. Since the set where $|x| = 1$ is compact, we may define $c_1 := \min_{|x|=1} V(x) > 0$ and $c_2 := \max_{|x|=1} V(x) > 0$ and get

$$c_1 |x|^2 = c_1 \leq V(x) \leq c_2 = c_2 |x|^2, \quad \forall x \in \mathbb{R}^n : |x| = 1. \tag{29}$$

Consider now any $x \in \mathbb{R}^n \setminus \{0\}$ and pick any $i \in \mathcal{Q}$ such that $V(x) = x^\top P_i x$. Then $V(x) = |x|^2 (x/|x|)^\top P_i (x/|x|) = |x|^2 V(x/|x|)$, which may be used in (29) to get

$$c_1 |x|^2 \leq V(x/|x|) |x|^2 = V(x) \leq c_2 |x|^2, \quad \forall x \in \mathbb{R}^n \setminus \{0\} \tag{30}$$

Inequalities (30), together with $V(0) = 0$ (trivially implied by (26)) prove (28a).

Proof of SOS of (27b) $\implies$ (28b). For this proof we exploit the results in [35]. First, consider $x \in \mathcal{C}_\varepsilon$ such that $|x| = 1$ and V is differentiable at x. Then, proceeding as in the previous case, $S_i(x)$ in (27b) being SOS implies

$$\begin{aligned} x^\top (P_i A + A^\top P_i) x + \sum_{j=1}^{q} \mu_{ij}(x) x^\top (P_i - P_j) x \\ - \mu_{i0}(x) x^\top (M - \varepsilon I) x \leq -2\alpha x^\top P_i x. \end{aligned} \tag{31}$$

Now, using the notation in [35, Def. 4], consider any $i \in \alpha_V(x)$, where $\alpha_V(x)$ denotes the essentially active index set map, which is not empty and ensures $x^\top P_i x \geq x^\top P_j x$ for all $j \in \mathcal{Q}$ due to [35, Lemma 1]. Since V is differentiable at x by construction, then we have $\nabla V(x) = \nabla(x^\top P_i x) = 2P_i x$. Summarizing, we have $V(x) = x^\top P_i x$ by definition and $x^\top(M - \varepsilon I)x \leq 0$ because $x \in \mathcal{C}_\varepsilon$. Consider now (31) together with $x^\top(P_i - P_j)x \geq 0$ and $\mu_{ij}(x) \geq 0$, to get

$$\dot{V}(x) = x^\top(P_i A + A^\top P_i)x \leq -2\alpha x^\top P_i x = -2\alpha V(x).$$

Homogeneity of the system is then exploited, similarly to (30), to extend the result to almost all $x \in C_\varepsilon$, as to be proven.

Proof of SOS of (27c) and (27d) $\implies$ (28c). Consider $x \in \mathcal{D}$ such that $|x| = 1$. Then, polynomials $J_i(x), \Lambda_i(x)$ in (27c), (27d) being SOS implies that

$$\begin{aligned} &x^\top R P_i R x - \mathrm{e}^{-2\beta}\sum_{j=1}^{q}\lambda_{ij}(x)x^\top P_j x + \lambda_{i0}(x)x^\top M x \leq 0, \\ &\sum_{j=1}^{q}\lambda_{ij}(x) \leq 1. \end{aligned} \tag{32}$$

Now pick any pair $i, k \in \mathcal{Q}$ such that $V(x) = x^\top P_k x \geq x^\top P_j x$ for all $j \in \mathcal{Q}$ and $V(Rx) = (Rx)^\top P_i (Rx)$. Then we may use (32), together with $x^\top M x \geq 0$ (because $x \in \mathcal{D}$), and $\lambda_{ij}(x) \geq 0$ for all $i, j \in \mathcal{Q}$, to get

$$\begin{aligned} V(Rx) = x^\top R^\top P_i R x &\leq \mathrm{e}^{-2\beta}\sum_{j=1}^{q}\lambda_{ij}(x)x^\top P_j x \\ &\leq \mathrm{e}^{-2\beta}\sum_{j=1}^{q}\lambda_{ij}(x)x^\top P_k x \leq \mathrm{e}^{-2\beta}x^\top P_k x = \mathrm{e}^{-2\beta}V(x). \end{aligned}$$

Lastly, homogeneity is exploited once more to extend the result to any $x \in \mathcal{D}$, thus completing the proof. ■

Based on Lemma 4 we can now prove Proposition 1.

Proof of Proposition 1. We exploit inequalities (28) proven in Lemma 4, to establish the statement of the proposition.

First of all note that, using inequalities (28a), (28b) and following similar steps to the ones reported in the proof of Lemma 2, we obtain that $\langle v, Ax\rangle \leq -2\alpha V(x), \forall x \in \mathcal{C}_{\frac{\varepsilon}{2}}, \forall v \in \partial V(x)$. This, together with standard comparison theory (see, e.g., [36, Lemma 8.1]), implies that any flowing solution to (5)-(6) must be associated to a decrease of V with exponential rate 2α, therefore proving item (iv) of Assumption 1 whenever $\alpha > 0$. Moreover, (28b) directly implies (7) because $\alpha \geq 0$ and inequality (28c) directly implies (8) because $\beta \geq 0$. Finally, about item (ii), all quadratic functions are homogeneous of degree two, so the same holds for V in (26), and positive definiteness of V follows from (28a). Strong convexity is guaranteed when $P_i > 0$. Indeed, each quadratic function $V_i(x) := x^\top P_i x$ is strongly convex with parameter $\eta_i = 2\lambda_{\mathrm{m}}(P_i)$ in (2), and for each $x, y \in \mathbb{R}^n$ such that V is differentiable at x, with $i, k \in \mathcal{Q}$ satisfying $i \in \alpha_V(x)$ (this implies $\nabla V(x) = \nabla V_i(x)$ and $V(x) = V_i(x)$) and $V(y) = V_k(y)$ we have, from (2),

$$\begin{aligned} V(y) = V_k(y) &\geq V_i(y) \\ &\geq V_i(x) + \langle \nabla V_i(x), y - x\rangle + \frac{\eta}{2}|y - x|^2 \\ &= V(x) + \langle \nabla V(x), y - x\rangle + \frac{\eta}{2}|y - x|^2 \end{aligned}$$

where $\eta = \min_{i\in\mathcal{Q}} \eta_i = 2\min_{i\in\mathcal{Q}} \lambda_{\mathrm{m}}(P_i)$, which proves (4). This, in turn, is equivalent to (2) (as stated and proven in Remark 1), which implies strong convexity due to Lemma 1. □

Remark 5: One simpler certificate for the conditions in Assumption 1 for the max of quadratics function V in (26) could be obtained using constant multipliers, in place of the polynomial SOS multipliers in (27). In particular, we may simplify the constraints in the statement of Proposition 1 as follows

$$P_i - \sum_{j=1}^{q}\tau_{ij}(P_i - P_j) > 0, \tag{33a}$$

$$\begin{aligned} P_i A + A^\top P_i + \sum_{j=1}^{q}\mu_{ij}(P_i - P_j) \\ - \mu_{i0}(M - \varepsilon I) + 2\alpha P_i \leq 0, \end{aligned} \tag{33b}$$

$$R^\top P_i R - \mathrm{e}^{-2\beta}\sum_{j=1}^{q}\lambda_{ij}P_j + \lambda_{i0}M \leq 0. \tag{33c}$$

Equations (33) come from multiple applications of the (*lossy*) S-procedure, which is known to be a conservative technique, where the conditions (33) are sufficient but not necessary to prove (28). This proved to be an issue in many numerical examples. Indeed, when using constant multipliers, the iterative algorithm presented in the next section does not converge for any of the examples that we considered. •

V. An iterative algorithm to synthesize max of quadratics Lyapunov functions

Algorithm 1 Iterative algorithm to obtain a sum of squares certified max-quadratics Lyapunov function.

Initialize parameters: $\delta_{\min}$, h, $N_{\max}$;
repeat
  for $i \in \mathcal{Q}$ **do** ▷ **BEGIN(Initialization step)**
    $P_i = R^\top R / \lambda_{\max}(R^\top R)$, where $R \in \mathbb{R}^{n\times n}$ is chosen randomly; ▷ Initialize the max-quadratics function
  end for
  $\text{constr}_\alpha = \text{SOS}\{F_i, \mu_{ij}, \mu_{i0}\}$ from (27), $\quad \forall (i,j) \in \mathcal{Q}^2$;
  $(\alpha, \mu_{ij}) \leftarrow \texttt{solvesos}(\text{constr}_\alpha, -\alpha)$;
  $\text{constr}_\beta = \text{SOS}\{J_{\text{lin},i}, \Lambda_{\text{lin},i}, \lambda_{\text{lin},ij}, \lambda_{i0}\}$ from (34), $\quad \forall (i,j) \in \mathcal{Q}^2$;
  $(\beta_{\text{lin}}, \lambda_{\text{lin},ij}) \leftarrow \texttt{solvesos}(\text{constr}_\beta, \beta_{\text{lin}})$;
  $\lambda_{ij} = \lambda_{\text{lin},ij} / \beta_{\text{lin}}, \quad \forall (i,j) \in \mathcal{Q}^2$;
  Initialize iteration counter: $c = 0$;
  Initialize maximum increment norm: $\delta = 10^{-2}$; ▷ **END(Initialization step)**
  repeat
    $\text{constr}_{lin} = [\ 0 \le \tilde{\alpha} \le \delta,\ -\delta \le \tilde{\beta}_{\text{lin}} \le 0,\ |\tilde{P}_i| \le \delta,\ |\tilde{\mu}_{ij}| \le \delta,\ |\tilde{\lambda}_{\text{lin},ij}| \le \delta\ ]$; ▷ **BEGIN(Path following step)**
    $\text{constr}_{SOS} = \text{SOS}\{\tilde{F}_i,\ \tilde{J}_i,\ \Lambda_i,\ \mu_{ij} + \tilde{\mu}_{ij},\ \mu_{i0},\ \lambda_{ij} + \tilde{\lambda}_{ij},\ \lambda_{i0}\}$ from (35), $\quad \forall (i,j) \in \mathcal{Q}^2$;
    $\tilde{P}_i \leftarrow \texttt{solvesos}([\text{constr}_{SOS}, \text{constr}_{lin}, (P_i + \tilde{P}_i) > 0], -\tilde{\alpha} + \tilde{\beta}_{\text{lin}})$;
    if (problem is not feasible) **then**
      break; ▷ If for numerical reasons the linearization is not feasible, quit the current iteration
    else
      $P_i^+ = (P_i + \tilde{P}_i) / \max_j \sigma_M(P_j + \tilde{P}_j)$; ▷ **END(Path following step)**
      $(\alpha^+, \mu_{ij}^+) \leftarrow \texttt{solvesos}(\text{constr}_\alpha, -\alpha)$, where $P_i = P_i^+$; ▷ **BEGIN(Verification step)**
      $(\beta_{\text{lin}}^+, \lambda_{\text{lin},ij}^+) \leftarrow \texttt{solvesos}(\text{constr}_\beta, \beta_{\text{lin}})$, where $P_i = P_i^+$;
      if (a problem is not feasible) **then**
        $(\alpha^+, \beta_{\text{lin}}^+, \tau_{ij}^+, \mu_{ij}^+, (\lambda_{\text{lin},ij})^+) = (\alpha, \beta_{\text{lin}}, \tau_{ij}, \mu_{ij}, \lambda_{\text{lin},ij})$; ▷ All the parameters remain unchanged
        $\delta^+ = \delta/2$; ▷ Approximation is too big: reduce the maximum increment norm
      else
        $\delta^+ = 1.1 \cdot \delta$; ▷ Approximation is good enough: try to increase the maximum increment norm
        if $|\alpha^+ - \alpha| < h$ and $|\beta_{\text{lin}}^+ - \beta_{\text{lin}}| < h$ **then**
          $c^+ = c + 1$; ▷ Count how many times in a row α and β_{lin} change of less than h
        else
          $c^+ = 0$;
        end if
      end if ▷ **END(Verification step)**
      $\lambda_{ij}^+ = \lambda_{\text{lin},ij}^+ / \beta_{\text{lin}}^+$;
    end if
  until $\delta < \delta_{\min}$ or $c \ge N_{\max}$ ▷ Exit the current iteration when the upper bound on the increment norm becomes less than $\delta_{\min}$, or $\alpha, \beta_{\text{lin}}$ did not change by more than h for $N_{\max}$ times in a row
until $\alpha > 0$ and $\beta_{\text{lin}} \le 1$ ▷ Run the algorithm with a new initialization, until it gives acceptable values for α, β
$\beta = -\ln(\beta_{\text{lin}})/2$;

As discussed in Remark 4, the conditions in (27) correspond to a semi-definite program only when the matrices P_i or the polynomial multipliers are fixed. In this section, we formulate an iterative algorithm to progressively improve α and β, based on the local linearization of (27), inspired by the path following algorithm to solve BMIs presented in [25].

The algorithm, which is summarized in Algorithm 1, reported at page 9, is divided into three main steps: initialization, path following and verification. The three steps are described in more detail hereafter.

The notation SOS$\{f_i, g_i\}$ means that we require the polynomials $f_i(x), g_i(x)$ to be SOS, for all $i \in \mathcal{Q}$.

Initialization step. The algorithm starts with a random choice of q positive definite matrices P_i. The random initialization is due to the fact that the optimization problem is not necessarily convex, so we use the Monte Carlo method to increase the

chances that a global minimum (or a good approximation of it) is found. After this choice, we can retrieve the maximum value for α, β such that we can solve SOS$\{\Lambda_i, F_i, J_i, \mu_{ij}, \mu_{i0}, \lambda_{ij}, \lambda_{i0}\}$. To do so, we first perform the change of variable $\beta_{\text{lin}} = \mathrm{e}^{-2\beta}$, then, to avoid the bilinear terms $\beta_{\text{lin}}\lambda_{ij}(x)$ in (27c), we equivalently reformulate (27d) and (27c) as

$$\Lambda_{\text{lin},i}(x) = \beta_{\text{lin}} - \sum_{j=1}^{q} \lambda_{\text{lin},ij}(x) + r_{i\Lambda}(x)(1 - x^\top x); \tag{34a}$$

$$\begin{aligned} J_{\text{lin},i}(x) = &-x^\top R^\top P_i R x + \sum_{j=1}^{q} \lambda_{\text{lin},ij}(x) x^\top P_j x \\ &- \lambda_{i0}(x) x^\top M x + r_{iJ}(x)(1 - x^\top x). \end{aligned} \tag{34b}$$

Since all the P_i's are fixed, the polynomials $F_i(x), J_{\text{lin},i}(x), \Lambda_{\text{lin},i}(x)$ are linear, because the decision variables are only α, β and the polynomial multipliers (see the discussion in Remark 4). We can then solve SOS$\{F_i, \mu_{ij}, \mu_{i0}\}$ maximizing α, and SOS$\{\Lambda_{\text{lin},i}, J_{\text{lin},i}, \lambda_{\text{lin},ij}, \lambda_{i0}\}$ minimizing β_{lin}. This gives us a feasible initial condition for the algorithm, where $\lambda_{ij} = \lambda_{\text{lin},ij}/\beta_{\text{lin}}$. Note that, in view of Proposition 1, we use positive definite matrices P_i, and the SOS requirement on polynomials $S_i(x)$ is automatically satisfied.

Path following step. Starting from a feasible solution obtained from the previous step, we can rewrite polynomials (27a)-(27c) using an incremental form (nominal value plus increment). Then we construct convex approximate conditions by imposing a bound on the increments and neglecting the bilinear terms. The explicit expression for the approximated incremental polynomials $\tilde{F}_i$, $\tilde{J}_i$ (where we drop the dependance on x of the polynomial multipliers) is

$$\begin{aligned} \tilde{F}_i(x) := &-x^\top \big((P_i + \tilde{P}_i)A + A^\top (P_i + \tilde{P}_i)\big)x \\ &- \sum_{j=1}^{q} \Big(\big(\mu_{ij} + \tilde{\mu}_{ij}\big) x^\top (P_i - P_j) x + \mu_{ij} x^\top (\tilde{P}_i - \tilde{P}_j) x \Big) \\ &+ \mu_{i0} x^\top (M - \varepsilon I) x + r_{iF}(1 - x^\top x) \\ &- 2(\alpha + \tilde{\alpha}) x^\top P_i x - 2\alpha x^\top \tilde{P}_i x, \end{aligned} \tag{35a}$$

$$\begin{aligned} \tilde{J}_i(x) := &-x^\top R^\top (P_i + \tilde{P}_i) R x + (\beta_{\text{lin}} + \tilde{\beta}_{\text{lin}}) \sum_{j=1}^{q} \lambda_{ij} x^\top P_j x \\ &+ \beta_{\text{lin}} \sum_{j=1}^{q} \big(\tilde{\lambda}_{ij} x^\top P_j x + \lambda_{ij} x^\top \tilde{P}_j x \big) \\ &- \lambda_{i0} x^\top M x + r_{iJ}(1 - x^\top x), \end{aligned} \tag{35b}$$

whereas Λ_i in (27d) remains unchanged because it does not involve bilinear terms. Note that some of the polynomial multipliers, e.g. $\mu_{i0}(x)$, are not decomposed incrementally, because they are not involved in any bilinear term. Solving SOS$\{\Lambda_i, \tilde{F}_i, \tilde{J}_i, \mu_{ij} + \tilde{\mu}_{ij}, \mu_{i0}, \lambda_{ij} + \tilde{\lambda}_{ij}, \lambda_{i0}\}$, while imposing that the increments have norms smaller than a selected value δ, we obtain a new Lyapunov function, which improves the initial values of α and β_{lin} by minimizing the objective function $obj(\tilde{\alpha}, \tilde{\beta}_{\text{lin}}) = -\tilde{\alpha} + \tilde{\beta}_{\text{lin}}$, under the additional constraints $\tilde{\alpha} \geq 0, \tilde{\beta}_{\text{lin}} \leq 0$. This ensures that the algorithm never selects optimization directions leading to worse values of α and β_{lin}. However, this solution is designed for the approximate problem and should be verified on the original conditions in the verification step below.

Verification step. Since the path following step provides an approximate solution, it is necessary to verify the exact conditions (27). Using the increments $\tilde{P}_i$ from the previous step, we fix $P_i^+ = \chi^{-1}(P_i + \tilde{P}_i)$, where the normalization factor $\chi = \max_j \lambda_{\text{M}}(P_j + \tilde{P}_j)$ ensures that $P_i^+ \leq I, \forall i \in \mathcal{Q}$ and helps numerically, without affecting feasibility, due to the homogeneity of (27). In particular, the feasibility of the SOS requirement is checked in *Yalmip* [37] by analyzing the numerical residuals when expressing a given polynomial through sums of squared terms. The problem is then feasible if these residuals are smaller than some tolerance $0 < \varepsilon_{\text{num}} \ll 1$. Moreover, strict inequalities are not supported, therefore some constraints like positive definiteness are expressed using the same tolerance, e.g. $P_i \geq \varepsilon_{\text{num}} I$.

After the normalization, we can solve the same problem we described in the initialization step, which is once again a semi-definite program.

If this step fails, then the maximum increment norm δ is reduced, otherwise it is increased.

Overall algorithm. We summarize the above-commented iterations in the pseudo-code shown in Algorithm 1. There, the instruction `solvesos`$\big(\text{constr}, f(x)\big)$ is consistent with the instruction defined by *Yalmip*, so it minimizes $f(x)$ subject to constr, which is a set of constraints including SOS requirements.

We now discuss some examples of reset-controlled systems, for which the iterative algorithm provides a max of quadratics Lyapunov function that satisfies Assumption 1. For these examples we also provide comparison between the hybrid solutions and the continuous-time solutions with (9), for various values of γ.

Example 1: In this example, we consider an unstable first-order reset element (FORE) performing set-point regulation of of a plant consisting of an integrator (see, e.g., [5]): according to the structure in (5)-(6), the system can be described through the matrices

$$A := \begin{bmatrix} 0 & 1 \\ -b_c & a_c \end{bmatrix}, \quad R := \begin{bmatrix} 1 & 0 \\ 0 & 0 \end{bmatrix}, \quad M := \begin{bmatrix} 0 & 1 \\ 1 & 0 \end{bmatrix}.$$

where the state is given by $x = [-e\ x_c]^\top$, with e being the difference between the integrator (plant) output and the reference value. We consider a FORE with a mildly exponentially unstable eigenvalue in unit feedback, namely $a_c = 0.1, b_c = 1$.

We can show that it is not possible to select a unique quadratic Lyapunov function $V(x) = x^\top P x$ to certify the stability of this system. Indeed, defining $P = \left[\begin{smallmatrix} p_{11} & p_{12} \\ p_{12} & p_{22} \end{smallmatrix}\right] > 0$, the condition $\langle \nabla V(x), Ax \rangle < 0$ evaluated in $x_a = (0, 1)$ and $x_b = (-1, 0)$ would require both $p_{12} > 0$ and $p_{12} + 0.1 p_2 < 0$, which can not hold at the same time since $p_2 > 0$ for any positive definite matrix. Conversely, we can select a max of quadratics Lyapunov function $V(x)$, as defined in (26), that satisfies (27), where we select $\varepsilon = 10^{-3}$.

The iterative algorithm is initialized with $q = 2$ and $d = 2$, and the resulting max of quadratics Lyapunov function is identified by the matrices

$$P_1 := \left[\begin{smallmatrix} 0.927 & 0.260 \\ 0.260 & 0.073 \end{smallmatrix}\right], \quad P_2 := \left[\begin{smallmatrix} 0.607 & -0.050 \\ -0.050 & 0.130 \end{smallmatrix}\right].$$

Matrices P_i are all positive definite, with the smallest eigenvalue being $\lambda_1(P_1) \approx 3 \cdot 10^{-6}$, which is larger than the numerical tolerance (set to $\varepsilon_{\text{num}} = 10^{-6}$), and satisfy SOS$\{(27)\}$ with $\alpha \approx 0.280, \beta = 0$. Figure 1 shows the level set of the max of quadratics Lyapunov function, corresponding to $V(x) = 1$.

Figure 2 shows the evolution of the error e, starting from an initial condition $x_0 = [-1\ 0]^\top$, comparing the evolution obtained from the hybrid implementation to the evolution obtained from the soft-reset implementation in (9). As we can see, higher values of γ generate a continuous-time system whose solutions approach the continuous-time evolution of the hybrid trajectory.

Once we obtain the max of quadratics Lyapunov function from Algorithm 1, we can check the minimum value of γ that guarantees stability of (9), using that specific V. This can be done by exploring the unit circle (i.e. considering any x such that $x^\top x = 1$) and computing the minimum value γ such that $\langle v, f \rangle \leq 0$ for all $v \in \partial V(x)$ and all $f \in F(x)$ in (9). Then, we can extend the result to the whole state space $\mathbb{R}^n$ exploiting the homogeneity of the problem. These values γ are reported in Figure 3, as a function of the number q of quadratics used to run Algorithm 1. Note that γ does not appear anywhere in the algorithm, therefore its value can be computed only after each iteration and it is not the object of the optimization. As different executions of Algorithm 1 result in different selections of matrices P_i, the blue dots in Figure 3 correspond to the minimum values obtained over a certain number of executions. These values still do not characterize the actual stability limit for (9) in this example (see e.g. Figure 2, where values of γ below the ones identified with this method generate converging solutions). An alternative algorithm that aims at the minimization of γ is an interesting subject of future work. ∘

Remark 6: In Example 1 and in the following ones a hybrid implementation of the resetting scheme is effective only after introducing a time regularization mechanism (as described in [7, Section I] and references therein), in order to prevent non-converging, Zeno solutions. One of the advantages of performing the soft-reset implementation in (9) is that no time regularization is needed to ensure global exponential stability. •

Remark 7: A plot of the minimum value of γ obtained as a function of the value ε has not been included in the analysis. Indeed, numerical evidence shows that ε has negligible effects on the resulting value of γ, especially when compared with the significant effect of q reported in Figure 3. •

Example 2: Consider Example 2 in [38], where a second-order plant is controlled by a FORE. The example shows that an accurately tuned hybrid controller can induce a significant overshoot reduction in the plant step response. The specific case we consider here is the one where the bound on the control input is set to $\kappa_M = 5$. The system can be described as in (5)-(6), where the matrices[2] correspond to

$$A := \left[\begin{smallmatrix} -0.6 & 0.6 & -1 \\ -0.4 & 0.4 & 1 \\ 0 & -1 & -1 \end{smallmatrix}\right], \quad R := \left[\begin{smallmatrix} 1 & 0 & 0 \\ 0 & 1 & 0 \\ 0.062 & -4.818 & 0 \end{smallmatrix}\right],$$
$$M := \left[\begin{smallmatrix} -0.004 & -0.392 & -0.020 \\ -0.392 & 0.830 & 1.010 \\ -0.020 & 1.010 & 0 \end{smallmatrix}\right].$$

The iterative algorithm, run with $q = 3$ and $d = 2$, gives a max of quadratics Lyapunov function defined by the matrices

$$P_1 := \left[\begin{smallmatrix} 0.049 & 0.075 & 0.006 \\ 0.075 & 0.255 & 0.042 \\ 0.006 & 0.042 & 0.037 \end{smallmatrix}\right], \quad P_2 := \left[\begin{smallmatrix} 0.049 & 0.065 & 0.003 \\ 0.065 & 0.275 & 0.027 \\ 0.003 & 0.027 & 0.030 \end{smallmatrix}\right],$$
$$P_3 := \left[\begin{smallmatrix} 0.050 & 0.010 & -0.005 \\ 0.010 & 0.999 & 0.032 \\ -0.005 & 0.032 & 0.002 \end{smallmatrix}\right]$$

[2]Due to a typo in [38], one element of matrix A was reported with the opposite sign, and it is corrected in this example.

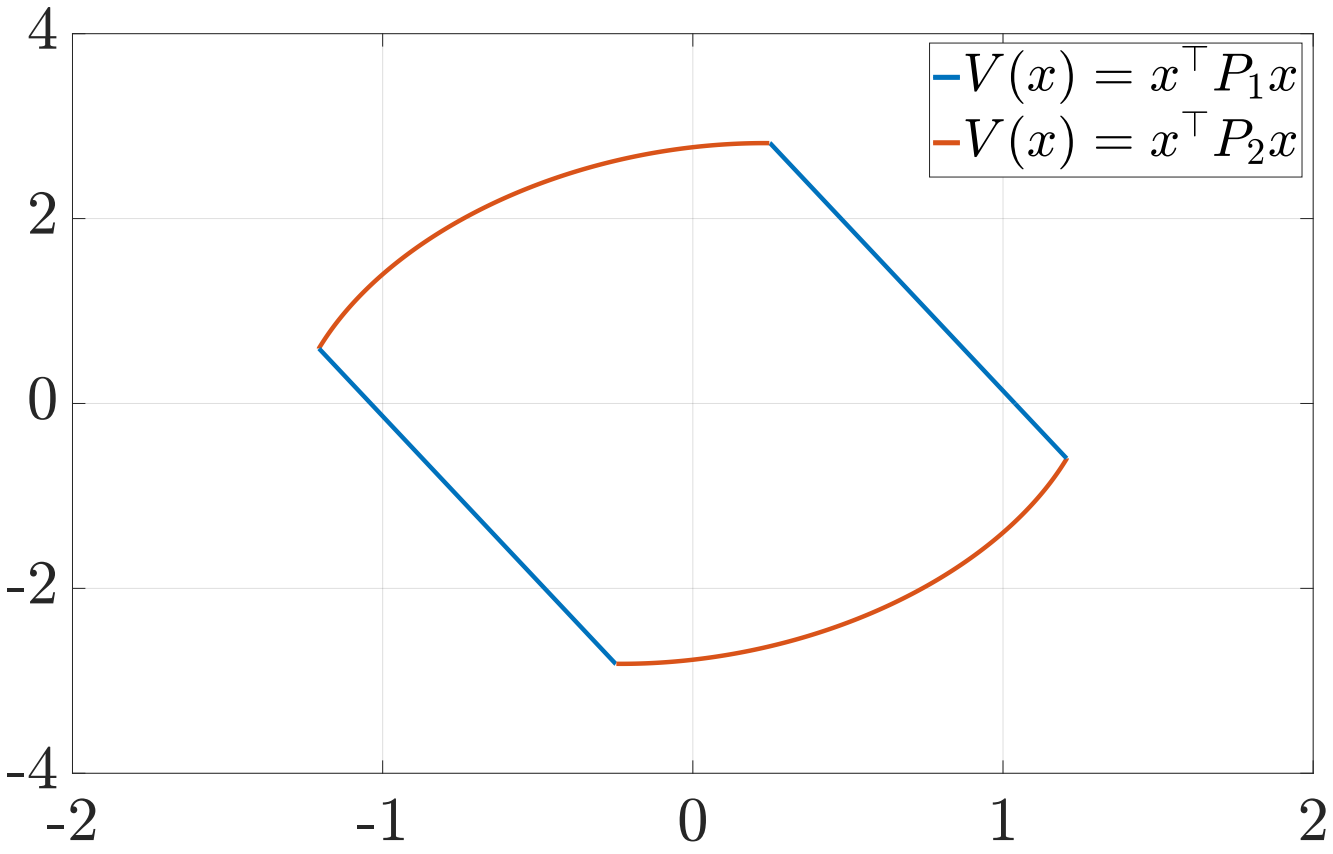

Fig. 1. Level set of the max of quadratics function in Example 1, corresponding to $V(x) = 1$.

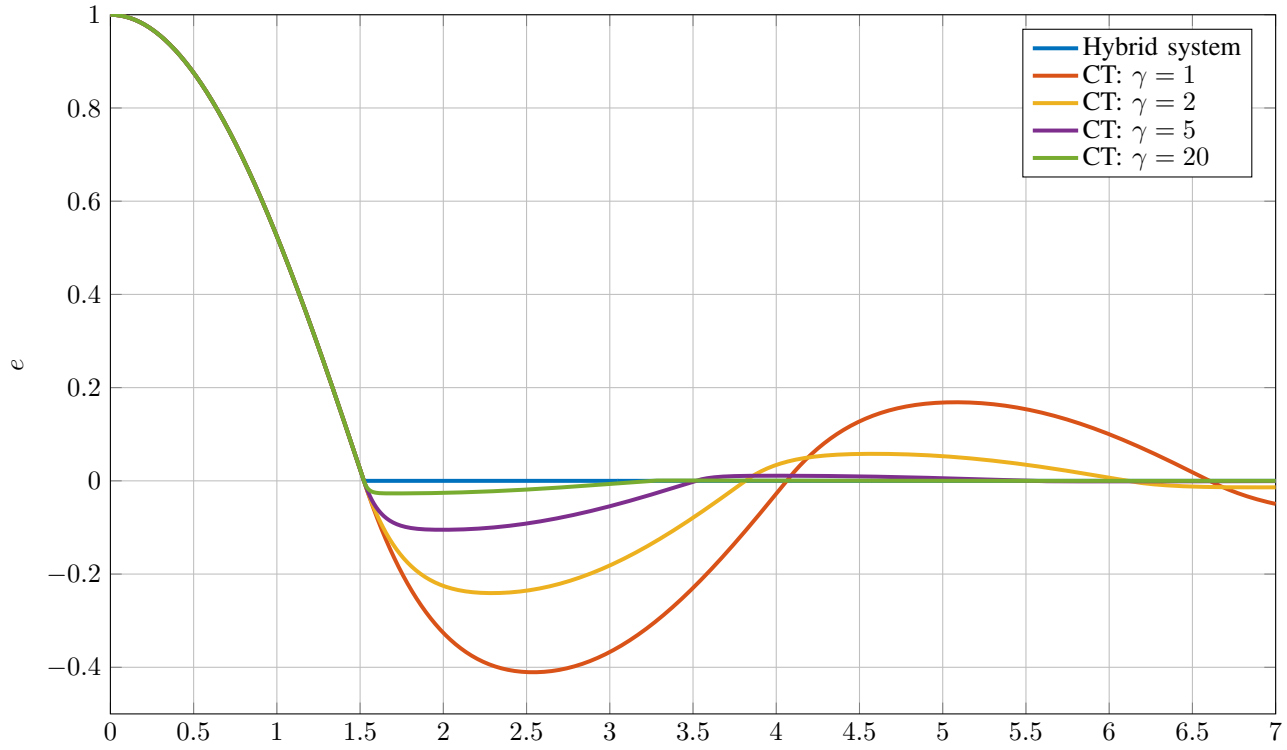

Fig. 2. Evolution of the output error for Example 1, hybrid implementation and CT implementation for different values of γ.

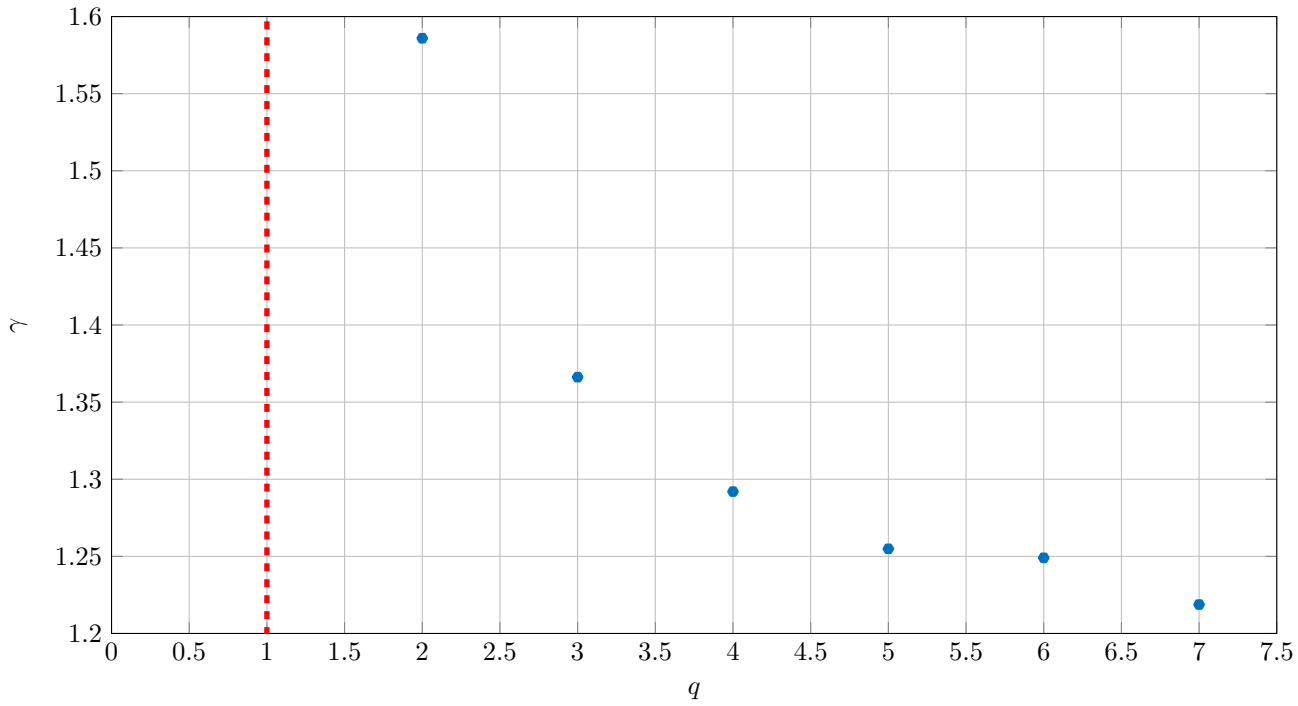

Fig. 3. Minimum value γ that certifies stability of (9) in Example 1, using the Lyapunov function obtained from Algorithm 1, as a function of q.

The matrices are all positive definite, with the smallest eigenvalue being $\lambda_1(P_3) \approx 6 \cdot 10^{-6}$, which is again larger than the numerical tolerance $\varepsilon_{\text{num}} = 10^{-6}$, and the resulting Lyapunov function satisfies SOS$\{(27)\}$ with $\alpha \approx 0.016, \beta = 0$. Figure 4 shows the level set of the max of quadratics Lyapunov function, corresponding to the points where $V(x) = 1$.

The evolution of the system output (corresponding to the second state of the closed loop) is reported in Figure 5. The evolution of the hybrid system (with time regularization) is once again compared to the evolution of the soft-reset implementation in (9) of this example, showing again that increasing values of γ lead to solutions approaching the continuous-time evolution of the hybrid feedback.

Algorithm 1 has been executed several times, and the minimum γ guaranteeing stability of the solutions of (9) has been identified for each execution. In Figure 6 these values of γ are plotted against the number q of quadratics used in the algorithm. ○

VI. Application to Reset Control of Certain Second-Order Mechatronic Systems

In many lightweight robotics applications, the plant dynamics can be expressed as an underdamped second order linear dynamical system, often with some input delay, see for example the experimental setup described in [39] or a precision positioning system analyzed, e.g., in [40]. While the control task for such systems is usually set-point regulation (or trajectory tracking), we can introduce an adaptive feedforward action in the controller, like in [41], and analyze the problem as a feedback stabilization one. Neglecting the pure time delay, which can be compensated for by using a Smith predictor, the plant dynamics can be described by the following state-space representation

$$\begin{aligned} \dot{x}_p &= A_p x_p + B_p u, \\ y_p &= [1\ 0] x_p \\ y_v &= [0\ 1] x_p, \end{aligned} \qquad A_p := \begin{bmatrix} 0 & 1 \\ -\omega_r^2 & -2\xi_s\omega_r \end{bmatrix}, \quad B_p := \begin{bmatrix} 0 \\ k\omega_r^2 \end{bmatrix}, \tag{36}$$

where $x_p \in \mathbb{R}^2$ includes the plant position y_p and the plant velocity y_v.

In considering an effective reset stabilizer for this system, let us look into the setting where we may use an accurate position measurement, to be considered for our continuous feedback, and a velocity measurement that should only be used as a trigger for the reset actions.

In particular, for the continuous-time feedback, we use a biproper controller with constant gain k_c and a phase lead induced by a pole-zero pair having the same time constant τ, with the pole $p_c = 1/\tau$ being unstable and the zero $z_c = -1/\tau$ being

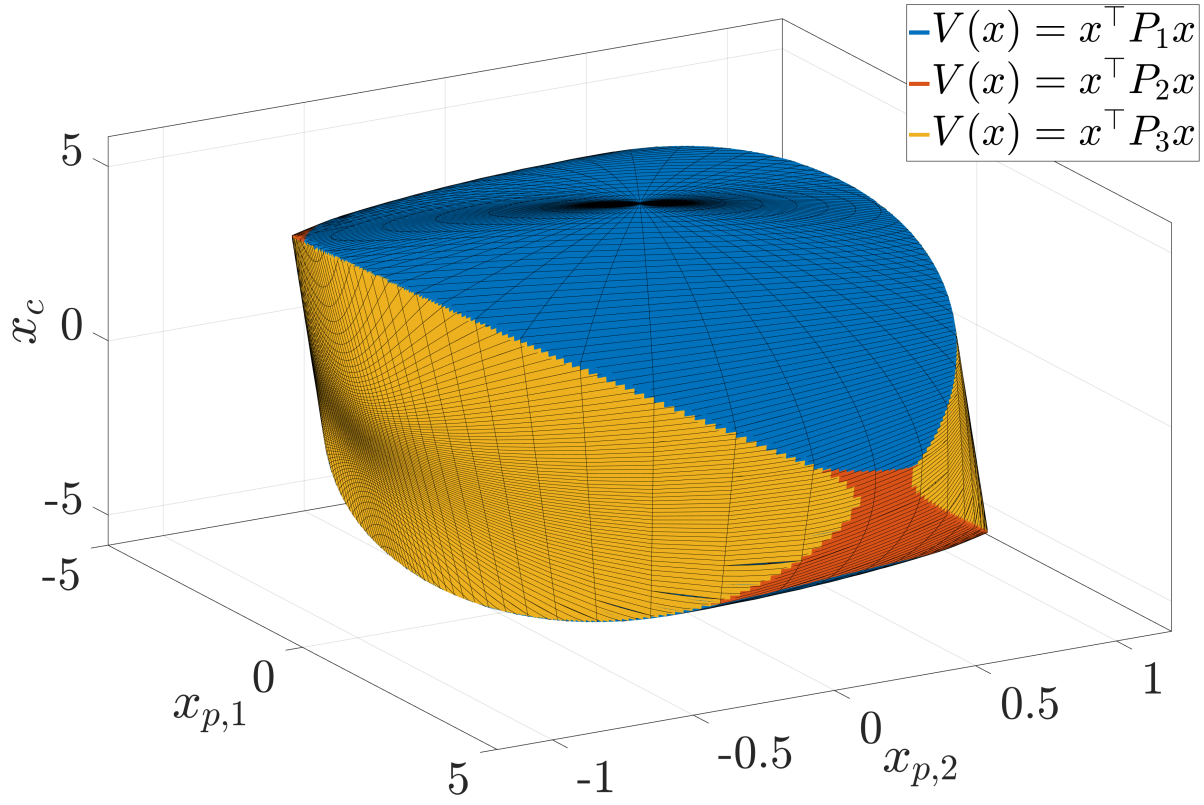

Fig. 4. Level set of the max of quadratics function in Example 2, corresponding to $\boldsymbol{V(x) = 1}$.

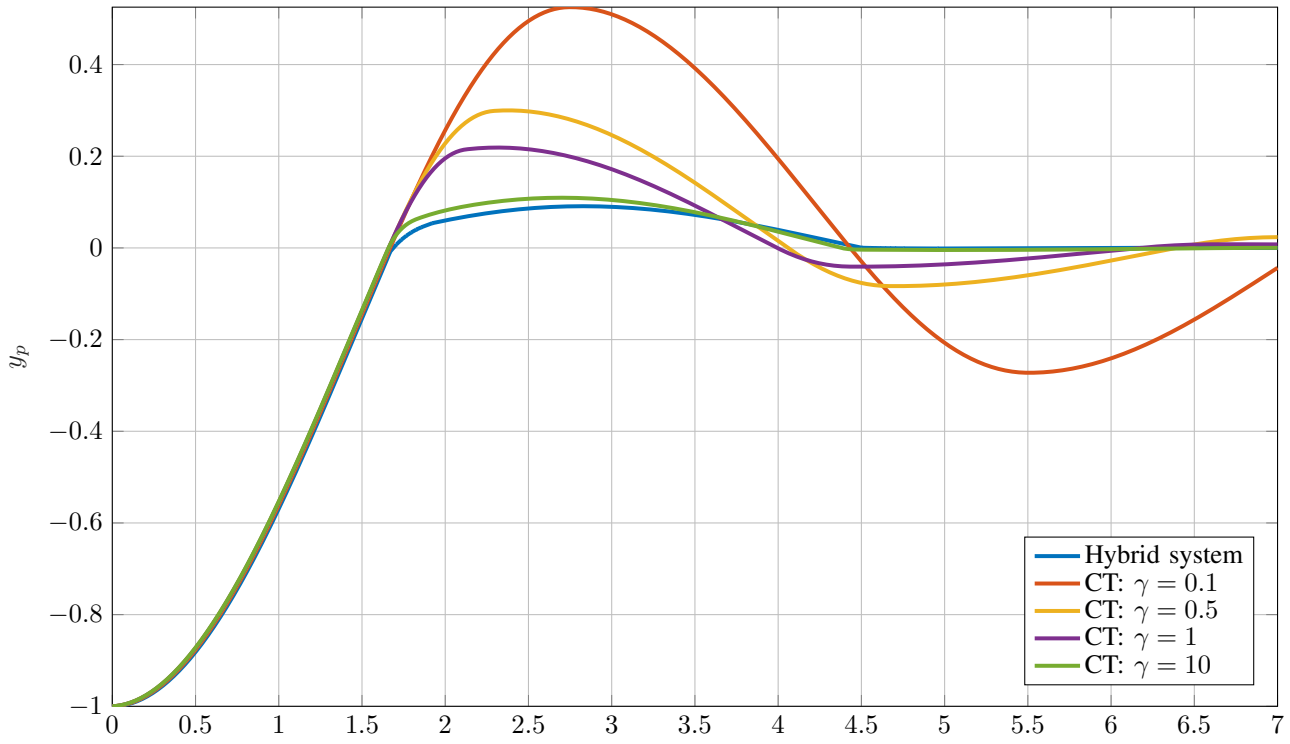

Fig. 5. Evolution of the plant output for Example 2, hybrid implementation and CT implementation for different values of γ.

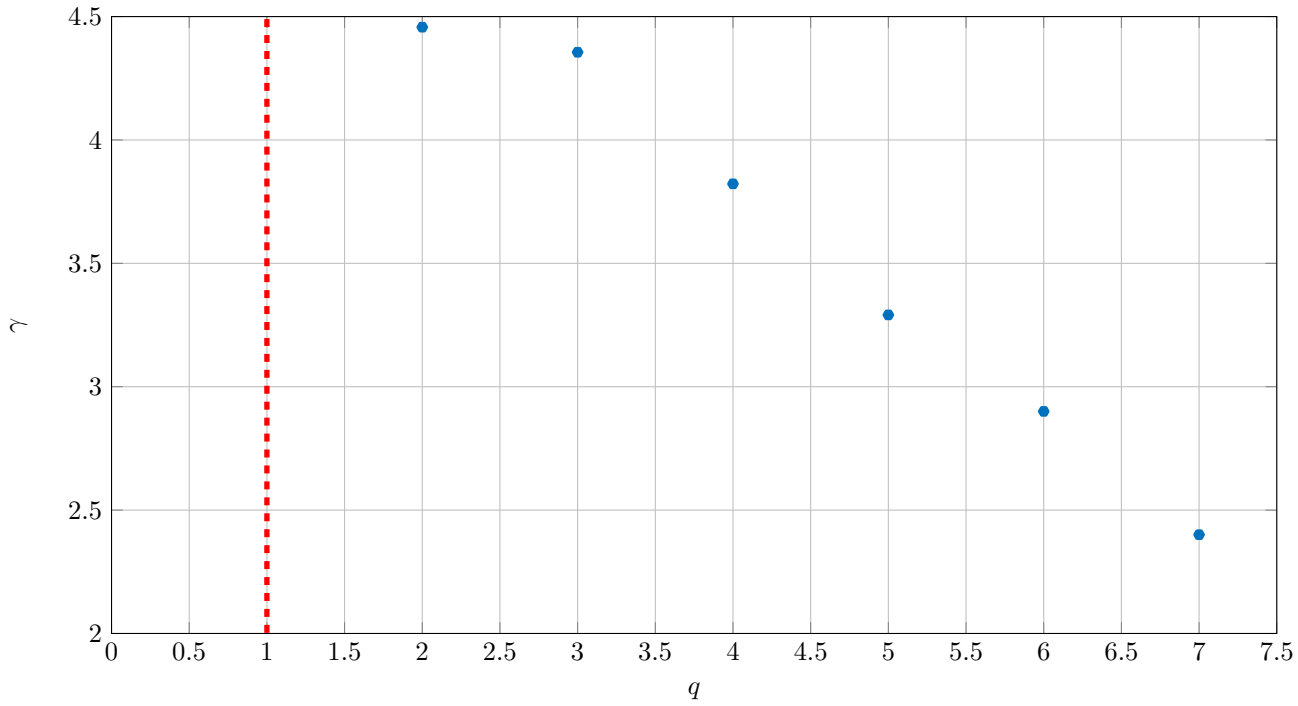

Fig. 6. Minimum value γ that certifies stability of (9) in Example 2, using the Lyapunov function obtained from Algorithm 1, as a function of $\boldsymbol{q}$.

minimum phase, namely $K(s) = k_c \frac{1+\tau s}{1-\tau s}$, whose state-space representation corresponds to

$$\begin{aligned} \dot{x}_c &= \frac{1}{\tau}\left(x_c - y_p\right), \\ u &= k_c\left(2x_c - y_p\right). \end{aligned} \tag{37}$$

The net continuous-time effect of this controller is to provide a pure phase lead without a constant effect k_c on the loop gain. The continuous-time component of this controller is only in feedback from the position measurement y_p.

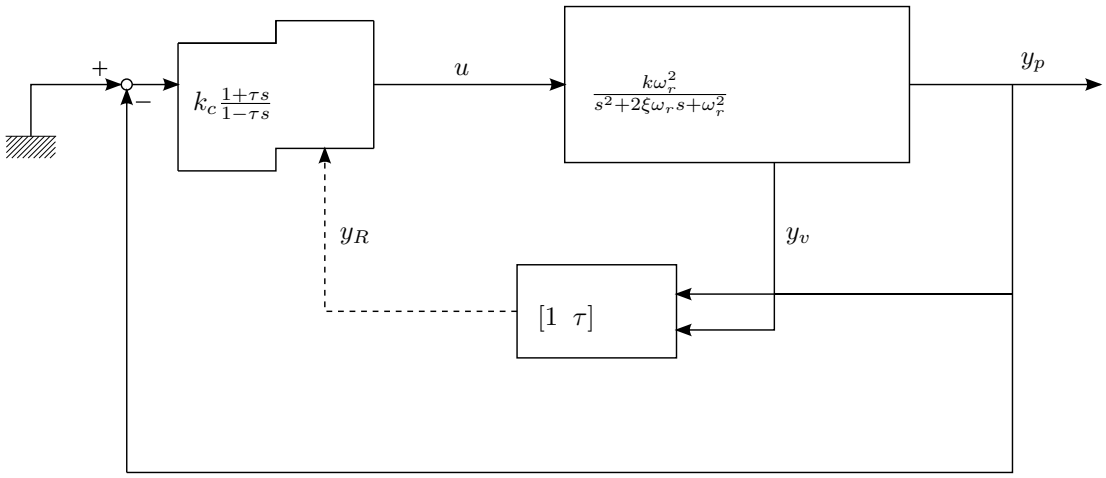

Fig. 7. Pure lead biproper reset filter proposed in Section VI.

To include suitable resetting actions on the biproper controller, we exploit the velocity measurement y_v in such a way to build the "reset" output defined as:

$$y_R := \tau y_v + y_p = [1 \ \tau] x_p, \tag{38}$$

which ensures that the transfer function between u and y_R be relative degree 1. Intuitively speaking, for this reset action, we virtually moved the minimum phase zero of $K(s)$ into the plant. Combining (36) with (37), the continuous dynamics state

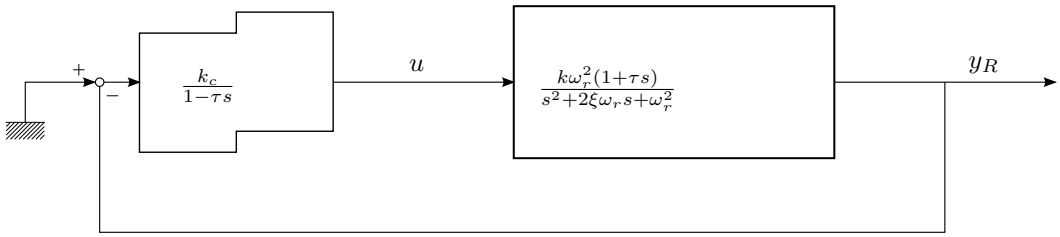

Fig. 8. Equivalent representation of the scheme in Figure 7 as a FORE in feedback with a minimum phase relative degree one plant.

matrix A of the closed-loop system in Figure 7, with state $x = (x_p, x_c)$, corresponds to (5)-(6) with

$$A := \left[\begin{array}{c|c} A_p - B_p k_c [1\ 0] & 2B_p k_c \\ \hline \left[-\frac{1}{\tau}\ \ 0\right] & \frac{1}{\tau} \end{array}\right], \tag{39}$$

and where R and M are to be chosen. Consider now selecting

$$R := \left[\begin{array}{c|c} I & 0 \\ \hline \left[\frac{1}{2}\ \ 0\right] & 0 \end{array}\right], \quad M := \left[\begin{array}{cc|c} -1 & -\tau/2 & 1 \\ -\tau/2 & 0 & \tau \\ \hline 1 & \tau & 0 \end{array}\right], \tag{40}$$

where R stems from $x_c^+ = y_p/2$ and M stems from jumping in the set where $y_R x_c \geq 0$. The motivation behind selection (40) is that we can perform a change of coordinates from $x = (x_p, x_c)$ to $\overline{x} = Tx$, where

$$T := \begin{bmatrix} 1 & 0 & 0 \\ 0 & 1 & 0 \\ -1 & 0 & 2 \end{bmatrix},$$

so as to obtain the following description (in the $\overline{x}$ coordinates):

$$\begin{aligned} \overline{A} &:= \left[\begin{array}{c|c} A_p & B_p \\ \hline \left[-\frac{1}{\tau}\ -1\right] & \frac{1}{\tau} \end{array}\right], \\ \overline{R} := \left[\begin{array}{c|c} I & 0 \\ \hline 0 & 0 \end{array}\right], &\qquad \overline{M} := \left[\begin{array}{c|c} 0 & \left[\frac{1}{\tau}\right] \\ \hline [1\ \tau] & 0 \end{array}\right], \end{aligned} \tag{41}$$

where $\overline{A} = TAT^{-1}$, $\overline{R} = TRT^{-1}$ and $\overline{M} = T^{-\top}MT^{-1}$. Using a block diagram representation, we may interpret (41) as rewriting the scheme in Figure 7 as a feedback interconnection between a relative degree 1 minimum phase second-order plant (this corresponds to the dynamics from u to y_R) and a first-order reset element having an unstable pole at $\frac{1}{\tau}$ and a loop gain k_c, as shown in Figure 8. We may then include a time regularization mechanism, and conclude from [7, Theorem 2] global exponential stability of the origin for the reset system (39), (40) if k_c is chosen large enough.

Notice that the jump and flow dynamics of this closed loop correspond to an output feedback control law only using y_p, however the knowledge of the velocity output y_v is required only to trigger jumps (notably, a similar setting was present in the work [42]).

While [7, Theorem 2] provides a guarantee that a large enough k_c exists ensuring global exponential stability of the origin, no immediate tools are available to determine that value. Here we use the plant parameters given in [40], using non-SI measurement units to obtain numerically balanced state matrices; namely, the parameters are expressed using millimeters, milliseconds and grams. Moreover, we select the controller parameters somewhat arbitrarily as $\tau = 1\text{ms}$ and $k_c = 10^{-2}\text{g}/\text{ms}^2$. Then we check global exponential stability using our Theorem 1 and Algorithm 1.

Running the algorithm with $q = 3$ and $d = 2$, gives a max of quadratics Lyapunov function defined by the matrices

$$P_1 := \begin{bmatrix} 0.444 & 0.084 & -0.415 \\ 0.084 & 0.084 & -0.064 \\ -0.415 & -0.064 & 0.671 \end{bmatrix}, \quad P_2 := \begin{bmatrix} 0.126 & 0.002 & 0.045 \\ 0.002 & 0.158 & 0.251 \\ 0.045 & 0.251 & 0.413 \end{bmatrix},$$
$$P_3 := \begin{bmatrix} 0.424 & 0.081 & -0.389 \\ 0.081 & 0.094 & -0.043 \\ -0.389 & -0.043 & 0.666 \end{bmatrix}.$$

The matrices are all positive definite, with the smallest eigenvalue being $\lambda_1(P_2) \approx 3 \cdot 10^{-5}$, which is larger than the numerical tolerance. The constraints SOS$\{(27)\}$ are satisfied by the resulting Lyapunov function, with $\alpha \approx 0.02$ and $\beta = 0$. Figure 9 shows the unit level set of the Lyapunov function, corresponding to the points where $V(x) = 1$.

Figure 10 shows the continuous-time evolution of the plant position for different simulation scenarios. The evolution of the hybrid closed loop with time regularization (blue) is compared to the evolution of the soft-reset implementation in (9) for different values of γ. It is possible to see that the trajectories of the sof-reset implementation appear increasingly similar to the trajectories of the hybrid reset system for increasing values of γ.

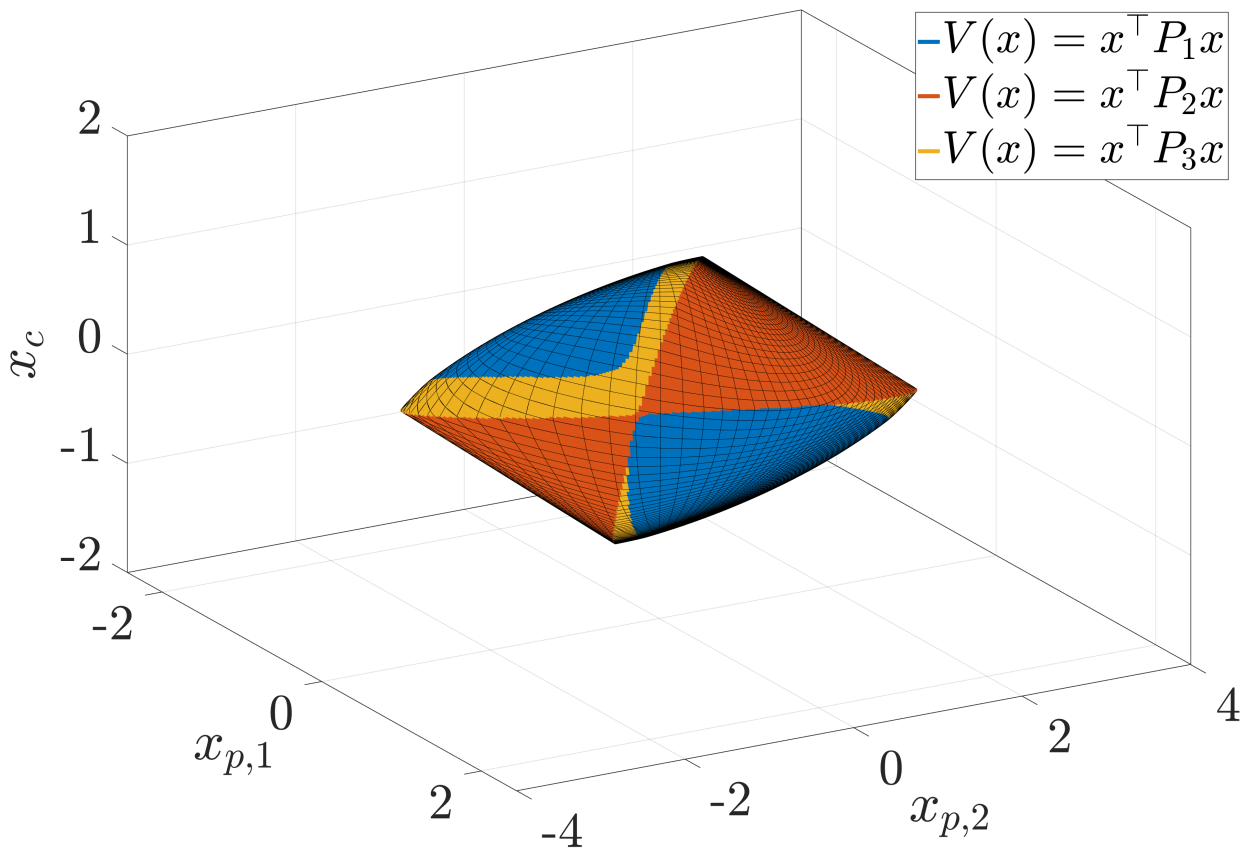

Fig. 9. Level set of the max of quadratics function for the precision positioning system, corresponding to $\boldsymbol{V(x) = 1}$.

VII. Conclusions

In this work we presented a soft-reset control paradigm, where an arbitrarily chosen positive scalar regulates how close the resulting closed-loop evolutions are to the flowing behaviour with the original hybrid controller. We proved asymptotic stability properties of the proposed control scheme, which in the original hybrid scheme can be obtained only through the introduction of time regularization. The proof relied on the use of nonsmooth Lyapunov functions, which led to the formulation of sufficient BMI conditions based on strongly convex max-of-quadratics Lyapunov functions with polynomial multipliers. We also proposed a numerical iterative algorithm which synthesizes such max-of-quadratics functions. The effectiveness of the numerical method was proved through its application to different examples and a case study stemming from mechatronic systems. Future work includes establishing stability conditions not requiring strong convexity, thereby allowing for more general Lyapunov certificates, proposing alternative design algorithms explicitly characterizing (and possibly optimizing) the minimum stabilizing gain γ and investigating a possible relation between the piecewise quadratic formulation and the original reset control flow and jump sets.

Acknowledgements: The authors would like to thank Milan Korda for the helpful tips on SOS programming.

References

[1] J. C. Clegg. A nonlinear integrator for servomechanisms. *Transactions of the American Institute of Electrical Engineers*, 77(1):41–42, 1958.
[2] I. Horowitz and P. Rosenbaum. Non-linear design for cost of feedback reduction in systems with large parameter uncertainty. *International Journal of Control*, 21(6):977–1001, 1975.
[3] A. Baños and A. Barreiro. *Reset control systems*. Springer, 2011.
[4] C. Prieur, I. Queinnec, S. Tarbouriech, and L. Zaccarian. Analysis and synthesis of reset control systems. *Found. & Trends in Syst. and Contr.*, 6(2-3):117–338, 2018.
[5] O. Beker, C.V. Hollot, and Y. Chait. Plant with an integrator: an example of reset control overcoming limitations of linear feedback. *IEEE Transactions Automatic Control*, 46:1797–1799, 2001.
[6] G. Zhao, D. Nešić, Y. Tan, and C. Hua. Overcoming overshoot performance limitations of linear systems with reset control. *Automatica*, 101:27–35, 2019.
[7] D. Nesic, A.R. Teel, and L. Zaccarian. Stability and performance of SISO control systems with first-order reset elements. *IEEE Transactions on Automatic Control*, 56(11):2567–2582, 2011.

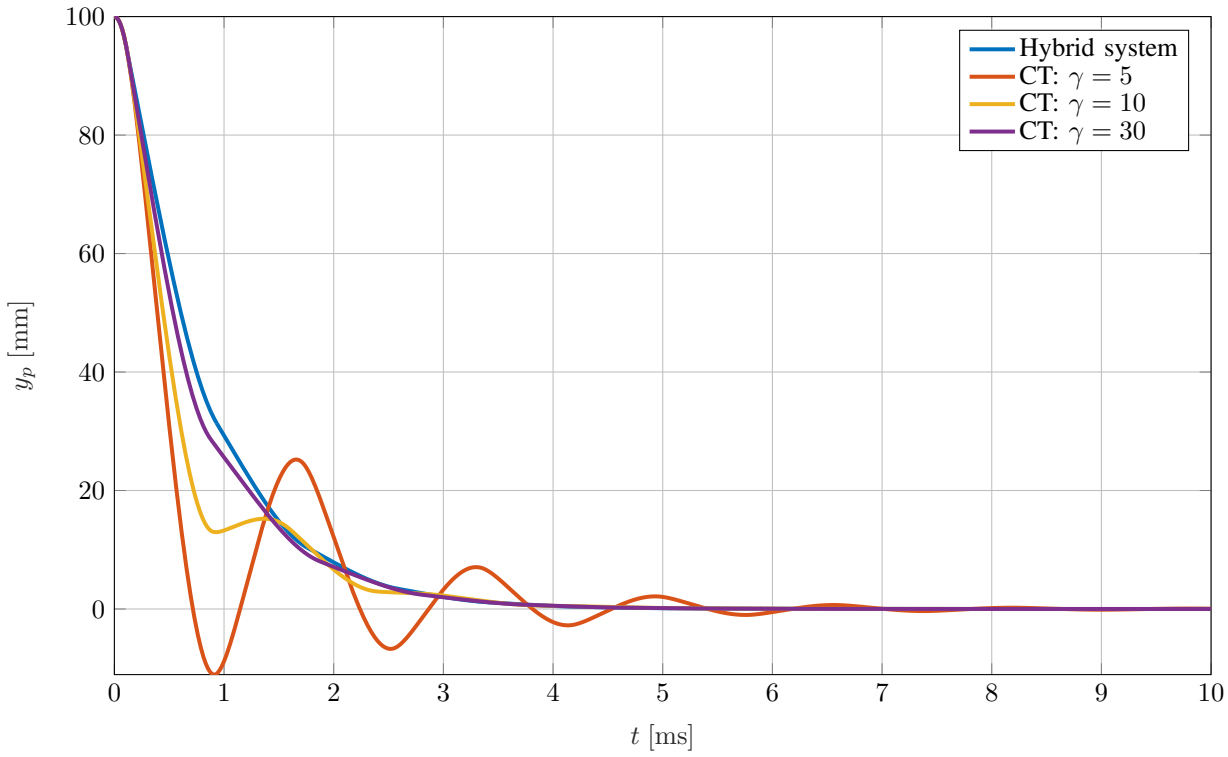

Fig. 10. Evolution of the precision positioning system output, hybrid implementation and CT implementation for different values of γ.

[8] L. Zaccarian, D. Nešić, and A.R. Teel. Analytical and numerical Lyapunov functions for SISO linear control systems with first-order reset elements. *Int. J. Robust. Nonlinear Control*, 21:1134–1158, 2011.

[9] C. Prieur, S. Tarbouriech, and L. Zaccarian. Lyapunov-based hybrid loops for stability and performance of continuous-time control systems. *Automatica*, 49(2):577–584, 2013.

[10] S.J.L.M. Van Loon, K.G.J. Gruntjens, M.F. Heertjes, N. van de Wouw, and W.P.M.H. Heemels. Frequency-domain tools for stability analysis of reset control systems. *Automatica*, 82:101–108, 2017.

[11] J. Zheng, Y. Guo, M. Fu, Y. Wang, and L. Xie. Improved reset control design for a PZT positioning stage. In *IEEE International Conference on Control Applications*, pages 1272–1277, 2007.

[12] A. Fernandez, A. Barreiro, A. Banos, and J. Carrasco. Reset control for passive teleoperation. In *34th Annual Conference of IEEE Industrial Electronics*, pages 2935–2940, 2008.

[13] D. Wu, G. Guo, and Y. Wang. Reset integral-derivative control for HDD servo systems. *IEEE Transactions on Control Systems Technology*, 15(1):161–167, 2007.

[14] H. Li, C. Du, Y. Wang, and Y. Guo. Discrete-time optimal reset control for hard disk drive servo systems. *IEEE Transactions on Magnetics*, 45(11 Part 1):5104–5107, 2009.

[15] J. Bakkeheim, T.A. Johansen, Ø.N. Smogeli, and A.J. Sørensen. Lyapunov-based integrator resetting with application to marine thruster control. *IEEE Transactions on Control Systems Technology*, 16(5):908–917, 2008.

[16] Y. Guo, Y. Wang, L. Xie, and J. Zheng. Stability analysis and design of reset systems: Theory and an application. *Automatica*, 45(2):492–497, 2009.

[17] F.S. Panni, H. Waschl, D. Alberer, and L. Zaccarian. Position regulation of an EGR valve using reset control with adaptive feedforward. *IEEE Transactions on Control Systems Technology*, 22(6):2424–2431, 2014.

[18] L. Chen, N. Saikumar, and S.H. HosseinNia. Development of robust fractional-order reset control. *IEEE Transactions on Control Systems Technology*, 28(4):1404–1417, 2019.

[19] Nima Karbasizadeh and S. Hassan HosseinNia. Continuous reset element: Transient and steady-state analysis for precision motion systems. *Control Engineering Practice*, 126:105232, 2022.

[20] Daniel Andreas Deenen, Bardia Sharif, Sebastiaan van den Eijnden, Hendrik Nijmeijer, Maurice Heemels, and Marcel Heertjes. Projection-based integrators for improved motion control: Formalization, well-posedness and stability of hybrid integrator-gain systems. *Automatica*, 133:109830, 2021.

[21] A.R. Teel. Continuous-time implementation of reset control systems. In Z.P. Jiang, C. Prieur, and A. Astolfi, editors, *Trends in Nonlinear and Adaptive Control – A tribute to Laurent Praly for his 65th birthday*, Lecture Notes in Control and Information Sciences 488, chapter 2, pages 27–41. Springer, 2021.

[22] Justin H. Le and Andrew R. Teel. Passive soft-reset controllers for nonlinear systems. In *60th IEEE Conference on Decision and Control (CDC)*, pages 5320–5325, 2021.

[23] F. Forni and A.R. Teel. Stability for a class of homogeneous hybrid systems by annular Lyapunov analysis. In *49th IEEE Conference on Decision and Control (CDC)*, pages 3289–3294, 2010.

[24] M. Della Rossa, R. Goebel, A. Tanwani, and L. Zaccarian. Piecewise structure of Lyapunov functions and densely checked decrease conditions for hybrid systems. *Mathematics of Control, Signals, and Systems (MCSS)*, 33:123–149, 2021.

[25] A. Hassibi, J. How, and S. Boyd. A path-following method for solving BMI problems in control. *Proceedings of the 1999 American Control Conference (Cat. No. 99CH36251)*, 1999.

[26] Y. Nesterov. *Introductory Lectures on Convex Optimization: A Basic Course*. Springer, 2004.

[27] F.H. Clarke. *Optimization and Nonsmooth Analysis*. Society for Industrial and Applied Mathematics, 1990.

[28] Xingyu Zhou. On the Fenchel duality between strong convexity and Lipschitz continuous gradient, 2018.

[29] F.H. Clarke, Y.S. Ledyaev, R.J. Stern, and P.R. Wolenski. *Nonsmooth analysis and control theory*, volume 178 of *Graduate Texts in Mathematics*. Springer, 1998.
[30] H. Nakamura, Y. Yamashita, and H. Nishitani. Smooth Lyapunov functions for homogeneous differential inclusions. In *Proceedings of the 41st SICE Annual Conference*, volume 3, pages 1974–1979, 2002.
[31] E.P. Ryan. An integral invariance principle for differential inclusions with applications in adaptive control. *SIAM J. Cont. Opt.*, 36(3):960–980, May 1998.
[32] J.J. Moreau and M. Valadier. A chain rule involving vector functions of bounded variation. *Journal of Functional Analysis*, 74(2):333–345, 1987.
[33] F.M. Ceragioli. *Discontinuous ordinary differential equations and stabilization*. PhD thesis, Univ. Firenze, Italy, 2000. Available online: `http://porto.polito.it/2664870/`.
[34] D. Nešić, A.R. Teel, G. Valmorbida, and L. Zaccarian. Finite gain $\mathcal{L}_p$ stability for hybrid dynamical systems. *Automatica*, 49:2384–2396, 2013.
[35] M. Della Rossa, A. Tanwani, and L. Zaccarian. Max-Min Lyapunov functions for switched systems and related differential inclusions. *Automatica*, 120:109123, 2020.
[36] João P. Hespanha. *Linear Systems Theory*. Princeton Press, Princeton, New Jersey, 2009.
[37] J. Löfberg. Yalmip : A toolbox for modeling and optimization in Matlab. In *In Proceedings of the CACSD Conference*, Taipei, Taiwan, 2004.
[38] C. Prieur, S. Tarbouriech, and L. Zaccarian. Improving the performance of linear systems by adding a hybrid loop. *IFAC Proceedings Volumes*, 44(1):6301–6306, 2011.
[39] M. Bolignari, G. Rizzello, L. Zaccarian, and M. Fontana. Smith-predictor-based torque control of a rolling diaphragm hydrostatic transmission. *IEEE Robotics and Automation Letters*, 6(2):2970–2977, 2021.
[40] N. Saikumar, R.K. Sinha, and S.H. HosseinNia. "Constant in gain lead in phase" element – application in precision motion control. *IEEE/ASME Transactions on Mechatronics*, 24(3):1176–1185, 2019.
[41] M. Cocetti, S. Tarbouriech, L. Zaccarian, and M. Ragni. A hybrid adaptive inverse for uncertain SISO linear plants with full relative degree*. *2019 American Control Conference (ACC)*, 2019.
[42] F. Fichera, C. Prieur, S. Tarbouriech, and L. Zaccarian. LMI-based reset H-infinity design for linear continuous-time plants. *IEEE Transactions on Automatic Control*, 61:1–1, 12 2016.

Riccardo Bertollo receiveid his Bachelor's degree in Industrial Engineering and his Master's degree in Mechatronics Engineering from the University of Trento (Italy) in 2017 and 2019, respectively. Since 2019 he has been a Ph.D. student in Mechatronics Engineering at the University of Trento. His research interests include the design and stability analysis of hybrid dynamical systems, with applications to mechatronic systems. In 2020, he was one of the finalists of the Young Author Best Paper Award at the 21st IFAC World Congress held in Berlin (DE). He is a Student member of the IEEE.

Andrew R. Teel received his A.B. degree in Engineering Sciences from Dartmouth College in Hanover, New Hampshire, in 1987, and his M.S. and Ph.D. degrees in Electrical Engineering from the University of California, Berkeley, in 1989 and 1992, respectively. After receiving his Ph.D., he was a postdoctoral fellow at the Ecole des Mines de Paris in Fontainebleau, France. In 1992 he joined the faculty of the Electrical Engineering Department at the University of Minnesota, where he was an assistant professor until 1997. Subsequently, he joined the faculty of the Electrical and Computer Engineering Department at the University of California, Santa Barbara, where he is currently a Distinguished Professor and director of the Center for Control, Dynamical systems, and Computation. His research interests are in nonlinear and hybrid dynamical systems, with a focus on stability analysis and control design. He has received NSF Research Initiation and CAREER Awards, the 1998 IEEE Leon K. Kirchmayer Prize Paper Award, the 1998 George S. Axelby Outstanding Paper Award, and was the recipient of the first SIAM Control and Systems Theory Prize in 1998. He was the recipient of the 1999 Donald P. Eckman Award and the 2001 O. Hugo Schuck Best Paper Award, both given by the American Automatic Control Council, and also received the 2010 IEEE Control Systems Magazine Outstanding Paper Award. In 2016, he received the Certificate of Excellent Achievements from the IFAC Technical Committee on Nonlinear Control Systems. He is Editor-in-Chief for Automatica, and a Fellow of the IEEE and of IFAC.

Luca Zaccarian received the Ph.D. degree from the University of Roma Tor Vergata (Italy) in 2000, where he has been Assistant and then Associate Professor until 2011. Since 2011 he is Directeur de Recherche at the LAAS-CNRS, Toulouse (France) and since 2013 he holds a part-time professor position at the University of Trento, Italy. His main research interests include analysis and design of nonlinear and hybrid control systems, modeling and control of mechatronic systems. He has been an associate editor for Systems and Control Letters and IEEE Transactions on Automatic Control. He is currently an associate editor for the IFAC journal Automatica. He was a nominated member of the Board of Governors of the IEEE-CSS in 2014, where he is an elected member in 2017–2019. He is a fellow of the IEEE since 2016. He was a recipient of the 2001 O. Hugo Schuck Best Paper Award given by the American Automatic Control Council.